AEDC-TR-73-52

OKB

AUG 1 1973

APR 22 1975

cy. 1

VISCOUS EFFECTS IN LOW-DENSITY NOZZLE FLOWS

David L. Whitfield

ARO, Inc.

June 1973

Approved for public release; distribution unlimited.

VON KÁRMÁN GAS DYNAMICS FACILITY

ARNOLD ENGINEERING DEVELOPMENT CENTER

AIR FORCE SYSTEMS COMMAND

ARNOLD AIR FORCE STATION, TENNESSEE

Property of U. S. Air Force
AEDC LIBRARY

NOTICES

When U. S. Government drawings specifications, or other data are used for any purpose other than a definitely related Government procurement operation, the Government thereby incurs no responsibility nor any obligation whatsoever, and the fact that the Government may have formulated, furnished, or in any way supplied the said drawings, specifications or other data, is not to be regarded by implication or otherwise, or in any manner licensing the holder or any other person or corporation, or conveying any rights or permission to manufacture, use, or sell any patented invention that may in any way be related thereto.

Qualified users may obtain copies of this report from the Defense Documentation Center.

References to named commercial products in this report are not to be considered in any sense as an endorsement of the product by the United States Air Force or the Government.

VISCOUS EFFECTS IN LOW-DENSITY NOZZLE FLOWS

David L. Whitfield
ARO, Inc.

Approved for public release; distribution unlimited.

FOREWORD

The work reported herein was conducted by the Arnold Engineering Development Center (AEDC) under the sponsorship of the Air Force Rocket Propulsion Laboratory (AFRPL), Air Force Systems Command (AFSC), under Program Element 62302F. This work was monitored by Captain Sam Thompson of AFRPL.

The results presented were obtained by ARO, Inc. (a subsidiary of Sverdrup & Parcel and Associates, Inc.), contract operator of the Arnold Engineering Development Center (AEDC), AFSC, Arnold Air Force Station, Tennessee. The work was conducted from March 9 to November 30, 1972, under ARO Project Nos. VY0202 and VC097. The manuscript was submitted for publication on January 18, 1973.

This technical report has been reviewed and is approved.

JIMMY W. MULLINS	A. L. COAPMAN
Lt Colonel, USAF	Colonel, USAF
Chief Air Force Test Director, VKF	Director of Test
Directorate of Test	

ABSTRACT

Viscous effects in low-density nozzle flows were investigated numerically, and comparisons were made with experimental data. The numerical method of Patankar and Spalding was modified to solve the internal laminar boundary-layer equations for two-dimensional flow or axisymmetric flow with or without transverse curvature. A listing is given of the computer code. Boundary-layer displacement thicknesses for typical nozzle geometries and flow conditions are presented. Solutions were obtained for specific conditions corresponding to experimental data. The result is a relatively fast, simple to use numerical procedure, which is shown to give results in good agreement with experimental data.

CONTENTS

APPENDIXES

Page

NOMENCLATURE

A	Cross-sectional area of nozzle
c_p	Specific heat at constant pressure
c_v	Specific heat at constant volume
d^*	Nozzle throat diameter
H	Local total enthalpy
$\overline{H}$	H/H_o
h	Heat-transfer coefficient
k	Thermal conductivity
M	Mach number
$\dot{m}$	Mass flux
Pr	Prandtl number, $\mu c_p/k$
p	Pressure
p_p	Measured pitot pressure
$\overline{p}$	$(\gamma - 1)p/(\gamma p_o)$
q_w	Nozzle wall heat-transfer rate
R	Longitudinal radius of curvature of converging portion of nozzle
$\overline{R}$	R/r^*
Re_{o,r^*}	Nozzle reservoir Reynolds number, $\rho_o(2H_o)^{1/2}r^*/\mu_o$

r	Defined by Eq. (4)
$\bar{r}$	r/r^*
r^*	Nozzle throat radius
T	Temperature
T_{aw}	Adiabatic wall temperature
$\bar{T}$	T/T_o
u	Velocity component in x direction
$\bar{u}$	$u/(H_o)^{1/2}$
v	Velocity component in y direction
$\bar{v}$	$v/(H_o)^{1/2}$
x	Coordinate along nozzle wall
$\bar{x}$	x/r^*
y	Coordinate normal to nozzle wall
$\bar{y}$	y/r^*
z	Coordinate along nozzle axis referenced to the throat
$\bar{z}$	z/r^*
α	Nozzle wall angle
γ	c_p/c_v
δ	Boundary-layer thickness defined as the value of y where $u/u_E = 0.99$
δ^*	Boundary-layer displacement thickness
ζ	Exponent in power law viscosity, $\mu \sim T^{\zeta}$
η	$\bar{y}/\bar{y}_E$
μ	Viscosity
$\bar{\mu}$	μ/μ_o
ν	Denotes planar or axisymmetric flow in Eq. (23)
ξ	Transformed x coordinate, Eq. (11)
ρ	Mass density
$\bar{\rho}$	ρ/ρ_o

ψ	Stream function
ω	Transformed stream function, Eq. (12)

SUPERSCRIPT

	Condition immediately downstream of a normal shock

SUBSCRIPTS

℄	Nozzle centerline
E	Outer edge of boundary layer
e	Nozzle exit
I	Inner edge of boundary layer
o	Reservoir (total) conditions
w	Nozzle wall

SECTION I
INTRODUCTION

Investigations of viscous effects in low-density gas flows in two-dimensional and axisymmetric channels and nozzles have been conducted during the past few years in support of the design of low-density wind tunnel facilities and small microthrust rockets used for spacecraft attitude control. In addition to these areas of interest, there are two other areas where attention to viscous effects is required. One is that of internal boundary-layer scaling. When the nozzle and/or plume flow of a rocket engine is to be investigated in a wind tunnel or space chamber, it is usually necessary to significantly reduce the size of the nozzle used. To achieve adequate simulation, the model nozzle viscous effects must appropriately simulate those of the actual rocket. A specific example of this problem is found in the laboratory study of rocket exhaust plumes interacting with the free-stream (Ref. 1). The other area of interest is associated with the study of gas dynamic and chemical lasers (Ref. 2). The total laser power output is influenced by the static gas pressure in the optical cavity just downstream of the nozzle exit. Since the nozzles used are small and since they operate at relatively high total temperatures, the nozzle viscous effects significantly influence the nozzle static pressure distribution. Although numerous comparisons with experimental data from low-density wind tunnel nozzles will be presented to check the accuracy of the results, the present investigation was motivated by the current interest in rocket nozzle scaling and the viscous effects on the operation of gas dynamic and chemical laser systems.

Some previous investigations of the design and analysis of low-density wind tunnel nozzles are given in Refs. 3 through 5. The method of Potter and Carden (Ref. 3) was developed to design nozzles for particular test section flow conditions. It is based on an integral technique which uses the similar solutions of Cohen and Reshotko (Ref. 6). Although the work of Potter and Carden (Ref. 3) has proved successful for the design of nozzles to produce desired flow conditions, it is not directly applicable to the analysis of specified nozzle geometry. Also, non-similar solutions presented in Ref. 4 indicate that similarity does not exist in nozzle flows, particularly near the throat, and as a consequence, inaccuracies may result from the use of similar solutions for relatively short nozzles.

The method presented in Refs. 4 and 5 solves the non-similar laminar boundary-layer equations with or without first-order transverse curvature (referred to as second-order in Refs. 4 and 7), with or without velocity slip and temperature jump boundary conditions, and it has been shown to be accurate. However, the method has certain disadvantages: (1) the numerical integration scheme is that of Jaffe, Lind, and Smith (Ref. 7) which requires a relatively large amount of computer time, (2) the computer program is large and not necessarily simple to use, (3) the transformation variables are not amenable to internal flow problems, and (4) large flow expansions frequently require interpolating the solutions, changing the numerical step size across the nozzle, and resuming the calculations. These disadvantages discourage the use of the method described in Refs. 4 and 5.

The methods described in Refs. 3 through 5 assume that the nozzle flow consists of a viscous region and an inviscid (core) region. Some previous investigations which are not restricted to such flows, but permit viscous effects across the entire channel, are described in Refs. 8 through 10. These investigations are more suitable for the study of flow in microthrust rockets where the flow may be fully viscous. However, these methods also have certain disadvantages for the present application. The works of Adams (Ref. 8) and Williams (Ref. 9) are based on similar solutions, the conditions for which are not likely to be satisfied by a large class of practical problems. The work of Rae (Ref. 10) is a significant contribution to the study of low-density nozzle flows, and this method will be discussed further in this report. Numerical results from Rae's method will be compared with results from Ref. 5, results obtained in the present investigation, and experimental data. Rae's method was shown to give good results for fully viscous flows (Ref. 10); however, it will be shown herein to be less accurate than the method of Refs. 4 and 5 or the present method for the flow regime of interest in this investigation.

The objectives of the present investigation are: (1) to provide results for estimating the viscous effects in low-density converging-diverging nozzle flows based on certain flow parameters and nozzle geometries, and (2) to provide a fast, simple to use method for calculating viscous effects in low-density nozzle flows. To meet these objectives, the numerical integration scheme of Patankar and Spalding (Ref. 11) was used. In fact, the program used for this work was taken directly from Ref. 11 and then suitably modified for internal, low-density flows. The resulting program is similar to that of Mayne (Ref. 2) except for the numerical scheme used near the wall. Also, the present work is based on a set of dimensionless equations which reduces the amount of input and provides more convenient solutions in the sense that they are applicable to flows which satisfy certain parameters rather than specific inputs of pressure, temperature, etc.

The following section describes the governing equations and boundary conditions, the variables used to nondimensionlize the equations, and the transformed equations. Section III describes briefly the numerical solution as well as some of the computational difficulties which have been encountered with this program. Section IV is devoted to numerical results and Section V to comparisons of the present results with previous theoretical investigations and experimental data. Some conclusions are given in Section VI.

SECTION II
BASIC EQUATIONS

The governing system of equations and the boundary conditions are presented in this section. Certain dimensionless and transformation variables are introduced and used to transform the governing equations for convenience of the numerical solution. Also, the boundary-layer displacement thickness is derived in the transformed plane. Although the program will solve the two-dimensional equations or axisymmetric equations with or without transverse curvature, only the equations appropriate to the latter with the transverse curvature terms retained are considered here in detail because they are more general. The two-dimensional equations can be obtained from the equations considered by setting $r \equiv 1$, and the axisymmetric equations without transverse curvature can be obtained by setting $r \equiv r_w$.

2.1 GOVERNING EQUATIONS

The governing system of equations is taken as that obtained by Probstein and Elliott (Ref. 12). The equations in curvilinear coordinates are:

Continuity Equation

$$\frac{\partial(\rho u r)}{\partial x} + \frac{\partial(\rho v r)}{\partial y} = 0 \tag{1}$$

Momentum Equation

$$\rho u \frac{\partial u}{\partial x} + \rho v \frac{\partial u}{\partial y} = -\frac{dp}{dx} + \frac{1}{r}\frac{\partial}{\partial y}\left(r\mu \frac{\partial u}{\partial y}\right) \tag{2}$$

Total Energy Equation

$$\rho u \frac{\partial H}{\partial x} + \rho v \frac{\partial H}{\partial y} = \frac{1}{r}\frac{\partial}{\partial y}\left\{ r\left[\frac{\mu}{Pr}\frac{\partial H}{\partial y} + \mu\left(1 - \frac{1}{Pr}\right) u \frac{\partial u}{\partial y}\right]\right\} \tag{3}$$

The total energy equation is obtained by multiplying the momentum equation by u and adding the result to the static energy equation. The coordinate system is defined in Fig. 1 (Appendix I) with the r(x, y) term defined for internal flow as

$$r(x,y) = r_w(x) - y \cos \alpha \tag{4}$$

Probstein and Elliott (Ref. 12) obtained Eqs. (1) through (3) by an order of magnitude analysis of the general forms of the continuity equation, Navier-Stokes momentum equations, and energy equation. The assumptions made in the analysis were that the ratio of the boundary-layer thickness to the longitudinal radius of curvature of the body surface was small compared to unity, and the ratio of the boundary-layer thickness to the nozzle radius was on the order of unity. Therefore, Eqs. (1) through (3) are valid for nozzles which have a longitudinal radius of curvature much larger than the nozzle radius. This stipulation is normally satisfied by axisymmetric convergent-divergent nozzles used for low-density wind tunnels, rockets, and gas dynamic and chemical laser systems.

The axisymmetric boundary-layer equations without transverse curvature terms correspond to those which can be obtained from Eqs. (1) through (3) by replacing r(x, y) with $r_w(x)$ as stated above. Because $r_w(x)$ is a function of x only, it can be eliminated from Eqs. (2) and (3), and therefore appears only in the continuity equation. The resulting set of equations can be used to describe internal or external boundary layers. It was shown in Ref. 5, by solutions with and without the transverse curvature terms, that the effect of transverse curvature is important for $\delta/r_w(x) \sim 0(1)$.

Implicit in Eq. (2) by the use of the total derivative of p with respect to x is the y component of the momentum equation as given by

$$-\frac{\partial p}{\partial y} = 0 \tag{5}$$

The validity of this equation is sometimes questioned for thick laminar boundary layers. However, the analysis of Probstein and Elliott (Ref. 12) indicates that this equation is consistent with the other equations in the governing set. Equation (5) was used in Refs. 4 and 5, and good agreement between calculated and measured boundary-layer profiles was obtained for flow conditions where 99 percent of the cross-sectional area of a nozzle was boundary layer.

For the boundary conditions at the edge of the boundary layer, it was assumed that an isentropic core flow exists along the nozzle centerline, from which the flow properties at the edge of the boundary layer can be calculated. The boundary conditions at the nozzle wall were taken as zero velocity and a prescribed wall temperature distribution or a prescribed wall heat-transfer distribution. Solutions were presented in Ref. 5 with and without velocity slip and temperature jump boundary conditions. For the conditions investigated in Ref. 5, it was found that the nozzle flow merged (that is, the boundary layer completely filled the nozzle) before velocity slip and temperature jump became significant. Therefore, no-slip wall boundary conditions were assumed adequate for this investigation.

The system of equations is completed by using the equation of state, $p = \rho RT$, and expressing the viscosity as some function of T, $\mu = \mu(T)$. The governing equations are next made dimensionless.

2.2 NONDIMENSIONALIZED EQUATIONS

Dimensionless variables are used to nondimensionalize the governing equations as follows:

$$\bar{x} = \frac{x}{r^*} \tag{6a}$$

$$\bar{y} = \frac{y}{r^*} \tag{6b}$$

$$\bar{r} = \frac{r}{r^*} \tag{6c}$$

$$\bar{\rho} = \frac{\rho}{\rho_o} \tag{6d}$$

$$\bar{H} = \frac{H}{H_o} \tag{6e}$$

$$\bar{\mu} = \frac{\mu}{\mu_o} \tag{6f}$$

$$\bar{p} = \frac{p}{\left(\frac{\gamma}{\gamma-1}\right)p_o} \tag{6g}$$

$$\bar{u} = \frac{u}{\left(H_o\right)^{1/2}} \tag{6h}$$

$$\bar{v} = \frac{v}{\left(H_o\right)^{1/2}} \tag{6i}$$

Using these equations in Eqs. (1) through (3) gives for the continuity, momentum, and total energy equation, respectively,

$$\frac{\partial(\bar{\rho}\,\bar{r}\,\bar{u})}{\partial\bar{x}} + \frac{\partial(\bar{\rho}\,\bar{r}\,\bar{v})}{\partial\bar{y}} = 0 \tag{7}$$

$$\bar{\rho}\,\bar{u}\frac{\partial\bar{u}}{\partial\bar{x}} + \bar{\rho}\,\bar{v}\frac{\partial\bar{u}}{\partial\bar{y}} = -\frac{d\bar{p}}{d\bar{x}} - \frac{(2)^{1/2}}{Re_{o,r^*}}\frac{1}{\bar{r}}\frac{\partial}{\partial\bar{y}}\left(\bar{r}\,\bar{\mu}\frac{\partial\bar{u}}{\partial\bar{y}}\right) \tag{8}$$

and

$$\bar{\rho}\,\bar{u}\frac{\partial\bar{H}}{\partial\bar{x}} + \bar{\rho}\,\bar{v}\frac{\partial\bar{H}}{\partial\bar{y}} = \frac{(2)^{1/2}}{Re_{o,r^*}}\frac{1}{\bar{r}}\frac{\partial}{\partial\bar{y}}\left\{\bar{r}\left[\frac{\bar{\mu}}{Pr}\frac{\partial\bar{H}}{\partial\bar{y}} + \bar{\mu}\left(1-\frac{1}{Pr}\right)\bar{u}\frac{\partial\bar{u}}{\partial\bar{y}}\right]\right\} \tag{9}$$

where

$$Re_{o,r^*} = \frac{\rho_o(2H_o)^{1/2}\,r^*}{\mu_o} \tag{10}$$

A few comments are in order concerning the choice of the dimensionless variables. Note that $(H_o)^{1/2}$ was used to normalize the velocity components u and v instead of the more commonly used maximum velocity $(2H_o)^{1/2}$. The motivation for this was to recover the same form of the boundary-layer equations in dimensionless variables as in physical plane variables. If $(2H_o)^{1/2}$ were used in Eqs. (6h) and (6i) in place of $(H_o)^{1/2}$, then the term $\bar{\mu}\,[1 - (1/Pr)]\bar{u}\,\partial\bar{u}/\partial\bar{y}$ in the right hand side of Eq. (9) would be $2\bar{\mu}\,[1 - (1/Pr)]\bar{u}\,\partial\bar{u}/\partial\bar{y}$, which would not be the same as in Eq. (3). The maximum velocity $(2H_o)^{1/2}$ was used in the definition of Re_{o,r^*} for convenience. This introduces the term $(2)^{-1/2}$ as a coefficient of Re_{o,r^*}, but since Re_{o,r^*} is a constant for each solution, the constant $(2)^{-1/2}$ causes no inconveniences in the numerical solutions. Note that by defining a new viscosity, $\mu = (2)^{1/2}\bar{\mu}/Re_{o,r^*}$, Eqs. (7) through (9) are identical to Eqs. (1) through (3). This, in fact, was done in the numerical computations.

For a given set of initial conditions, boundary conditions, γ, Pr, nozzle geometry, etc., the solution to Eqs. (7) through (9) depends only on Re_{o,r^*} if a power law viscosity variation with temperature is assumed, i.e., $\bar{\mu} = \bar{T}^{\zeta} = (T/T_o)^{\zeta}$. However, if, for example, Sutherland's viscosity law is assumed, then the solutions will also depend on the absolute value of temperature. Because the calculation of viscosity is carried out in a separate subroutine in the computer program, it is convenient to use any viscosity law desired. Solutions will be presented for both Sutherland's law and power law variations of viscosity.

2.3 TRANSFORMED EQUATIONS

Equations (7) through (9) were transformed from the dimensionless physical $\bar{x}$ - $\bar{y}$ plane to the ξ - ω plane by the transformation variables

$$\xi(\bar{x}) = \bar{x} \tag{11}$$

and

$$\omega(\bar{x},\bar{y}) = \frac{\psi(\bar{x},\bar{y}) - \psi_I(\bar{x})}{\psi_E(\bar{x}) - \psi_I(\bar{x})} \tag{12}$$

where $\psi(\bar{x},\bar{y})$ is the stream function which identically satisfies the continuity equation, Eq. (7), i.e.,

$$\frac{\partial\psi}{\partial\bar{x}} = -\bar{\rho}\,\bar{v}\,\bar{r} \tag{13}$$

and

$$\frac{\partial\psi}{\partial\bar{y}} = \bar{\rho}\,\bar{u}\,\bar{r} \tag{14}$$

The transformation used is that due to von Mises with ω introduced to restrict the integration across the boundary layer from zero to unity. The subscripts I and E denote the inner and outer edge of the boundary layer, respectively, and ψ_I and ψ_E are functions of $\bar{x}$ only. The operators $(\partial/\partial\bar{x})$ and $(\partial/\partial\bar{y})$ are given by

$$\frac{\partial}{\partial\bar{x}} = \frac{\partial}{\partial\xi} + \frac{\partial\omega}{\partial\bar{x}}\frac{\partial}{\partial\omega} = \frac{\partial}{\partial\xi} + \left(\frac{\partial\omega}{\partial\psi}\frac{\partial\psi}{\partial\bar{x}} + \frac{\partial\omega}{\partial\psi_I}\frac{d\psi_I}{d\bar{x}} + \frac{\partial\omega}{\partial\psi_E}\frac{d\psi_E}{d\bar{x}}\right)\frac{\partial}{\partial\omega} \tag{15}$$

and

$$\frac{\partial}{\partial\bar{y}} = \frac{\partial\omega}{\partial\bar{y}}\frac{\partial}{\partial\omega} = \frac{\partial\omega}{\partial\psi}\frac{\partial\psi}{\partial\bar{y}}\frac{\partial}{\partial\omega} \tag{16}$$

Using Eqs. (12) through (14) in Eqs. (15) and (16) and applying them to Eqs. (8) and (9) give for the momentum and total energy equations

$$\frac{\partial \bar{u}}{\partial \bar{x}} + \frac{\bar{r}_I \dot{m}_I + \omega\left(\bar{r}_E \dot{m}_E - \bar{r}_I \dot{m}_I\right)}{\psi_E - \psi_I} \frac{\partial \bar{u}}{\partial \omega} = \frac{(2)^{1/2}}{Re_{o,r^*}} \frac{\partial}{\partial \omega}\left[\frac{\bar{r}^2 \bar{\rho}\, \bar{u}\, \bar{\mu}}{(\psi_E - \psi_I)^2} \frac{\partial \bar{u}}{\partial \omega}\right] - \frac{1}{\bar{\rho}\, \bar{u}} \frac{d\bar{p}}{d\bar{x}} \tag{17}$$

and

$$\frac{\partial \bar{H}}{\partial \bar{x}} + \frac{\bar{r}_I \dot{m}_I + \omega\left(\bar{r}_E \dot{m}_E - \bar{r}_I \dot{m}_I\right)}{\psi_E - \psi_I} \frac{\partial \bar{H}}{\partial \omega} = \frac{(2)^{1/2}}{Re_{o,r^*}} \left\{\frac{\partial}{\partial \omega}\left[\frac{\bar{r}^2 \bar{\rho}\, \bar{u}\, \bar{\mu}}{(\psi_E - \psi_I)^2\, Pr} \frac{\partial \bar{H}}{\partial \omega}\right] + \frac{\partial}{\partial \omega}\left[\frac{\bar{r}^2 \bar{\rho}\, \bar{u}\, \bar{\mu}}{(\psi_E - \psi_I)^2}\left(1 - \frac{1}{Pr}\right) \frac{\partial(\bar{u}^2/2)}{\partial \omega}\right]\right\} \tag{18}$$

where

$$\frac{d\psi_I}{d\bar{x}} = -\bar{r}_I \dot{m}_I \tag{19}$$

and

$$\frac{d\psi_E}{d\bar{x}} = -\bar{r}_E \dot{m}_E \tag{20}$$

and where $\xi(\bar{x})$ has been replaced by $\bar{x}$. Except for the constant $(2)^{1/2}/Re_{o,r^*}$, Eqs. (17) and (18) are identical to the momentum and total energy equations for external flow which are solved numerically by the method of Patankar and Spalding (Ref. 11). The calculation of the mass transfer fluxes $\dot{m}_I$ and $\dot{m}_E$ will be discussed in Section III.

The boundary-layer displacement thickness was used to calculate an effective nozzle geometry which in turn was used to calculate an axial pressure distribution. The displacement thickness, δ^*, which takes into account transverse curvature is expressed by Probstein and Elliott (Ref. 12) as

$$\int_0^{\delta^*} 2\pi r\, \rho_E\, u_E\, dy = \int_0^{y_E} 2\pi r(\rho_E u_E - \rho u)dy \tag{21}$$

Solving Eq. (21) for δ^* gives

$$\frac{\delta^*}{r^*} = \frac{\bar{r}_w - \left[\bar{r}_w^{\,2} - 2\cos\alpha\left(\bar{y}_E\bar{r}_w - \frac{\bar{y}_E^{\,2}\cos\alpha}{2} - \frac{\psi_E - \psi_I}{\bar{\rho}_E\bar{u}_E}\right)\right]^{1/2}}{\cos\alpha} \tag{22}$$

A quadratic equation for δ^* must be solved to obtain Eq. (22) from Eq. (21). The positive sign was chosen so that $\delta^*/r^* < \bar{r}_w/\cos\alpha$. The displacement thicknesses for axisymmetric flows without transverse curvature and planar flows can be obtained by using $(r_w)^\nu$ in place of r in Eq. (21). The displacement thicknesses are then given by

$$\frac{\delta^*}{r^*} = \bar{y}_E - \frac{(\psi_E - \psi_I)}{(\bar{r}_w)^\nu\bar{\rho}_E\bar{u}_E} \tag{23}$$

where $\nu = 0$ for planar flows and $\nu = 1$ for axisymmetric flows without transverse curvature.

SECTION III
NUMERICAL SOLUTION

The numerical solution of Eqs. (17) and (18) is discussed in this section. The basic scheme is briefly described and a listing of the computer code is presented. A description of the necessary inputs to the program is given, and some computational difficulties which have been encountered with the program are discussed.

3.1 BASIC SCHEME

As previously stated, the basic numerical integration scheme of Patankar and Spalding (Ref. 11) was suitably modified and used to solve the governing internal flow equations pertinent to the present investigation. Because the flow regime of the present investigation was entirely laminar, some subroutines of the computer code listed in Ref. 11 which were associated with turbulent flow were removed for the present code. Also, most, but not all, statements pertaining to turbulent flow were removed. The computer code as used for the present investigation is listed in Appendix III. Essentially this same program was used on two different computers at AEDC, a Scientific Data Systems (SDS) 9300 and an International Business Machines (IBM) 370/155. The code in Appendix III is the one used on the IBM 370/155.

The basic numerical scheme used by Patankar and Spalding is discussed in detail in Ref. 11. One of the primary features of this finite difference technique is that the set of linear algebraic equations which must be solved has only three unknowns in each equation, and this set can be solved by simple successive substitution (Gauss reduction, or elimination, Ref. 13) rather than by matrix inversion. This technique provides a saving in computational time. For example, the time required to solve the algebraic equations by elimination (at a fixed $\bar{x}$ location) is proportional to the number of unknowns, whereas the time required to solve the equations by matrix inversion is proportional to the square of the number of unknowns (Ref. 13). On the IBM 370/155, a solution at a fixed $\bar{x}$ location required approximately 0.6 sec using 200 grid points across the boundary layer (ω direction) in single precision. The corresponding time required on the SDS 9300 was approximately 10 sec. The IBM 370/155 carried 8 digits in single precision, whereas the SDS 9300 carried 12.

The general method of solution consisted of matching the inviscid and viscous flow regions in the nozzle by iterating on the axial pressure distribution. An initial guess of the axial pressure distribution throughout the nozzle is made, and a solution is obtained. The displacement thickness calculated in this solution is used to obtain an effective nozzle geometry which in turn is used to calculate a new pressure distribution from one-dimensional, perfect gas, expansion theory. A typical iteration and convergence process is illustrated in Fig. 2. The use of one-dimensional perfect gas expansion theory as opposed to a method-of-characteristics solution, for example, seems justified on the basis of the agreement with experimental data in Section V. The same iteration process as used here and some suggestions for choosing the initial pressure distribution are discussed further by Whitfield and Lewis (Ref. 5).

The symbols and subroutines used in the Patankar and Spalding code are clearly defined and discussed in Ref. 11. Therefore, the remainder of this section is directed toward the modifications and additions which have been made to the code of Ref. 11.

3.2 INPUT CONDITIONS

The input requirements to this program are particularly simple. The input was modified somewhat from that of the original code (Ref. 11), and the input variables are described below in the order they are read-in in the present code (Appendix III).

SYMBOL	DESCRIPTION
KRAD	This input permits the treatment of plane flows and axisymmetric flows with first-order transverse curvature. Also, although not pointed out in Ref. 11, axisymmetric flows without transverse curvature can be treated by setting KRAD = 0. Plane flows can be treated by setting KRAD = 0 and $\overline{r}_w(\overline{x}) \equiv 1$ (or a constant). Axisymmetric flows including first-order transverse curvature are treated by setting KRAD = 1 (at least not zero) and using the actual geometry $\overline{r}_w(\overline{x})$.
IDIMEN	If the nozzle considered is two-dimensional, set IDIMEN = 0. This sets $\overline{r}_w(\overline{x}) \equiv 1$ in subroutine RAD. If the nozzle considered is axisymmetric set IDIMEN = 1.
NEQ	This is the number of partial differential equations to be solved. The code of Ref. 11 also includes the solution to the equation for the conservation of chemical species. However, this equation was never considered in this investigation and only the momentum and total energy equations were used, in which case NEQ = 2. The chemical species equation is, however, retained in the present code.
KEX	This input specifies the type of E boundary. It can be either 1, 2, or 3, according to whether the E boundary is a wall, free boundary, or a symmetry line, respectively. However, in the present investigation KEX was always 2, i.e., E was a free boundary, and certain modifications must be made to the present code if anything other than KEX = 2 is used.

KIN	This is similar to KEX except KIN specified the type of I boundary. For the present code KIN = 1 must be used; otherwise certain modifications must be made.
IHEAT	This is used in subroutine FBC and indicates a wall temperature boundary condition if IHEAT = 1 and a wall heat-transfer rate if IHEAT $\neq$ 1. In the present code, the only wall heat flux considered was zero, i.e., an adiabatic wall. If a heat flux other than zero is prescribed, then a few statements in subroutine SLIP must be modified (see Ref. 11). The only wall temperatute distribution considered in the present work was T_w/T_o = constant. However, subroutine FBC is easily modified to accommodate any desired variation of T_w.
N	This is the number of strips across the boundary layer, i.e., in the ω direction. It must always be at least three less than the dimensions of the arrays of the variables across the layer, e.g., the maximum N which can be used with the dimensions of the arrays in the present code is 197.
REØRS	Reservoir Reynolds number, Re_{o,r^*}.
ZETA	Exponent in the power law variation of viscosity with temperature, $\mu \sim T^{\zeta}$
PR(1)	Prandtl number, Pr
GAM	Ratio of specific heats, γ
ALPHA	Nozzle wall half-angle, α
XR	Longitudinal radius of curvature of the nozzle upstream of the throat, $\overline{R}$
XL	Termination condition for the computations, maximum value of $\overline{x}$
USUP	This input controls the location of the E boundary. It is associated with the entrainment rate and it will be discussed in the following subsection. USUP was varied from 0.99 to 0.999, and was usually 0.995.

YSTART	Initial velocity and total enthalpy profiles were calculated from the expressions $u/u_E = 2\eta - \eta^2$ and $H/H_o = H_w/H_o + [1-(H_w/H_o)]u/u_E$ where $\eta = \bar{y}/\bar{y}_E$ and $\bar{y}_E$ = YSTART. Suggestions for choosing YSTART will be given in the following subsection. A typical value of YSTART is 0.5.
TWTØ	Ratio of wall to total temperature, T_w/T_o
XSTEP	Specification of the integration step-size in the $\bar{x}$ direction in terms of local wall radius, e.g., step size, DX, is given by the product of XSTEP times $\bar{r}_w$. A typical value of XSTEP is 0.05.
LMAX	Number of $\bar{x}$ locations where an input pressure is specified.
XX(L)	Array of $\bar{x}$ locations where an input pressure is specified. Array goes from 1 to LMAX.
PØP(L)	Input pressure for corresponding $\bar{x}$ location, XX(L). Array goes from 1 to LMAX.

The last three inputs, LMAX, XX(L), and POP(L), are read-in in subroutine PRE, the other inputs are read-in in subroutine BEGIN.

Because of the nature of the process involved in iterating on the axial pressure distribution, it is important to input a smooth initial pressure distribution. For the present computations, the initial pressure distribution was calculated using the actual geometry at and upstream of the throat and some effective inviscid nozzle wall downstream of the throat. (Actually, the slope of the assumed inviscid nozzle wall just downstream of the throat was matched to the nozzle wall half-angle to produce a smooth wall in order to have a smooth pressure distribution.) The simple program used to calculate the initial pressure distribution for the present computations is included in Appendix IV for convenience of users where such an approximation is adequate. The particular version of the code presented in Appendix IV uses $\delta^* \sim x^{3/2}$ for axisymmetric nozzles and $\delta^* \sim x$ for two-dimensional nozzles. Although $\delta^* \sim x^{3/2}$ was not used to calculate the initial pressure distribution for all axisymmetric nozzle computations presented herein, it appears to provide a reasonable approximation to the variation of δ^* in axisymmetric nozzles.

Inasmuch as several wind tunnel and laser nozzles have conical sections downstream of the throat and constant longitudinal radius of curvature for the upstream converging portions, this general nozzle geometry (which can be sufficiently described by the inputs ALPHA and XR) was considered in this investigation. However, subroutine RAD can be easily modified to include any geometry, such as for example contoured nozzles which were analyzed in Ref. 5 using the same governing equations as used here.

3.3 SOME POSSIBLE COMPUTATIONAL DIFFICULTIES

The mass-transfer rate, or entrainment rate, across the E boundary essentially governs the location of the edge of the boundary layer. This technique of locating the edge of the boundary layer has certain advantages in analyzing low-density nozzle flows; however, it might also cause some difficulties if not handled correctly. The entrainment rate was calculated in the present investigation by evaluating the momentum equation, Eq. (17), along a constant ω line, denoted as ω_B, near the E boundary. This technique is discussed in Ref. 11. The scheme requires the specification of the velocity along $\omega = \omega_B$ (where ω_B was taken as 0.9) at the next downstream station. This velocity is denoted as $\tilde{u}_B$ and it is suggested in Ref. 11 that it be taken as $\tilde{u}_B = 0.99\,\overline{u}_E$, where $\overline{u}_E$ is the velocity at the edge of the boundary layer at the next downstream station. (Note that $\overline{u}_E$ can be calculated from the Euler equation since $d\overline{p}/d\overline{x}$ is presumed known for the particular iteration.) It was found in the present work, however, that more flexibility could be obtained with the program if $\tilde{u}_B$ was taken as $\tilde{u}_B = (USUP)\overline{u}_E$ and USUP was input for each solution. The quantity USUP provides a means of suppressing the outer edge of the boundary layer which is advantageous in treating flows which are nearly merged. For example, during the process of iterating on the axial pressure distribution, it was observed (Fig. 2, and also Ref. 5) that δ^* resulting from the first two iterations usually provided upper and lower bounds on the final converged δ^*. Therefore, if the flow is sufficiently rarefied, the pressure distribution resulting from the thinnest δ^* may be such that the following iteration would predict a merged flow when in fact the flow is not merged and could be calculated if a better guess for the initial pressure distribution could be made. In some cases the calculation of merged flow in the iteration process can be avoided by using a small value of USUP (a value of 0.99 is herein regarded as small and 0.999 is regarded as large) to suppress the edge of the boundary layer and prevent an indication of merging. The suppression seems to apply only to the outer edge of the layer and the calculated profiles over most of the layer remain essentially unchanged. For this reason, the converged δ^*, or pressure distribution, obtained using a small USUP usually differs by a small amount from that obtained using a larger USUP, say 0.995. After convergence is obtained using a small value of USUP a final solution can be obtained using a larger value. The value of 0.99 for $\tilde{u}_B/\overline{u}_E$ as suggested in Ref. 11 seems to excessively suppress the boundary layer for the present internal flow calculations. For most solutions reported herein, USUP was 0.995.

The step-size along the $\overline{x}$ component was taken for most of the solutions as 5 or 7.5 percent of the local wall radius. This step-size was sufficiently small for most problems. However, if calculations of properties in the nozzle throat region are of particular interest, such as the nozzle wall heat-transfer rate, a smaller step-size may be desirable.

In some applications where nozzle exit properties are of particular interest, it may be desirable to conserve computer time and use a relatively large $\overline{x}$ component step-size. For such problems some difficulties might be encountered in starting the solutions. Consider a finite-difference form of Eqs. (19) and (20)

$$(\psi_E - \psi_I)_D = (\psi_E - \psi_I)_U + (\overline{r}_I\dot{m}_I - \overline{r}_E\dot{m}_E)_U(\overline{x}_D - \overline{x}_U) \tag{24}$$

If Re_o, r^* and/or YSTART is small, then $(\psi_E\text{-}\psi_I)_U$ calculated from the initial profile will be small. Depending on the initial profiles and flow conditions, $\dot{m}_E$ may be positive for the first few stations and therefore $(\psi_E\text{-}\psi_I)_D$ could be less than $(\psi_E\text{-}\psi_I)_U$ for these first few stations and might even become negative. To circumvent this difficulty one could reduce the step-size $(\overline{x}_D\text{-}\overline{x}_U)$. However, if this is not desirable in view of computational time requirements, another approach is to increase YSTART in order to increase $(\psi_E\text{-}\psi_I)_U$ at the first station. The first few station solutions would consequently not be as accurate as solutions obtained by using a small $\overline{x}$ step-size. Therefore, although the solutions are started at the beginning of the converging portion of the nozzle upstream of the throat, this technique of increasing YSTART should be used with caution if accurate solutions (particularly properties which depend on derivatives near the wall such as heat-transfer rate) in the throat region are required. As stated previously, a typical value of YSTART was 0.5. The largest value of YSTART used to obtain solutions was unity, but this depends on XR.

Heat transfer and viscous effects change the effective nozzle throat from the location corresponding to the actual geometric nozzle throat. The subroutine NEWPPØ searches for the minimum effective nozzle radius and uses it for the throat in calculating a one-dimensional pressure distribution for the next iteration. However, if a sufficient number of solutions near the throat are not taken, then the true minimum area and its location used in calculating a new pressure distribution may not be accurately approximated. Then, the resulting $d\overline{p}/d\overline{x}$ in the throat region for the following iteration may not be smooth. In this case, the error in $d\overline{p}/d\overline{x}$ for each successive iteration would become worse. This is especially a problem in solutions for flows which have adiabatic or relatively hot nozzle walls. It is suggested that if the initial guess of the δ^* distribution is not a particularly good one, e.g., if the calculated δ^* at the exit is not within 20 to 30 percent of the assumed δ^*, then an improved pressure distribution should be calculated by the program in Appendix IV (or some similar method). This ensures a smooth pressure distribution, and since convergence is, in general, much faster in the throat region than further downstream where the relative displacement thicknesses are larger, few, if any, extra iterations are required.

Although areas have been pointed out where computational difficulties have been encountered with this program, it should also be pointed out that this numerical scheme is actually rather rugged, as for example compared to the method of Ref. 5. It is in general not sensitive to input conditions and seldom "blows up."

SECTION IV
NUMERICAL RESULTS

Solutions are presented in this section for typical nozzle configurations which provide some indication of the effect of Re_o, r^*, γ, Pr, ζ, T_w/T_o, α, transverse curvature, and two-dimensional versus axisymmetric flows. Table I (Appendix II) summarizes the conditions of the solutions presented in this section.

Of particular interest in nozzle flows is the displacement thickness, δ^*. By using δ^* and the nozzle geometry, an effective inviscid nozzle radius can be determined from which Mach number and other flow properties outside the boundary layer can be estimated. The displacement thicknesses for Conditions 1 to 8 of Table I are presented in Figs. 3 to 10.

Solutions were started at the beginning of the converging portion of the nozzles where $z/r^* = -3$. However, to conserve computing time, extremely small step-sizes were not utilized for all the solutions in this region (as discussed in Section III), and results are not presented in Figs. 3 to 10 for $z/r^* < -2$. Some solutions were repeated, however, with smaller step-sizes with no appreciable changes in the results presented.

At least for some values of Re_{o,r^*} in Figs. 3 to 7 and 9 to 10, negative displacement thicknesses were calculated in the throat region. This is due to the relatively cool wall increasing the gas density and hence the local mass flux near the wall. The adiabatic wall results presented in Fig. 8 do not indicate negative δ^* for the same flow conditions. Similar results concerning the calculation of negative δ^* have been reported previously, e.g., Potter and Carden (Ref. 3) and Whitfield and Lewis (Refs. 4 and 5).

Some indication of the effect of using various gases in a fixed nozzle geometry with fixed flow conditions is provided in Figs. 3 to 5. The specific heat ratio, Prandtl number, and power law viscosity variation with temperature of Figs. 3 to 5 closely approximate the properties of carbon dioxide (CO_2), helium (He), and nitrogen (N_2), respectively. For example, by considering the nozzle exit displacement thickness for $Re_{o,r^*} = 10^4$, one observes that, for the indicated flow conditions, δ^* using He is about 200 percent of that when using CO_2, and δ^* using N_2 is about 150 percent of that when using CO_2.

Results are presented in Figs. 5 and 6 for identical conditions except for the nozzle wall half-angle. Figure 5 has a wall half-angle of 10-deg, and Fig. 6 has a half-angle of 15 deg. For the same geometric area ratio, the expansion process is more rapid for the $\alpha = 15$ deg nozzle than the $\alpha = 10$ deg. Also, the nozzle wall length for the same area ratio is longer for the 10-deg nozzle than for the 15-deg nozzle. The result is to produce a larger exit δ^* for the 10-deg nozzle than for the 15-deg nozzle for the same geometric area ratio. For $Re_{o,r^*} = 3 \times 10^3$, the 10-deg nozzle exit δ^* is about 18 percent larger than that of the 15-deg nozzle.

It should be pointed out that although δ^* is relatively small because of the cool walls, δ is not necessarily small. For example, in Fig. 5 for $Re_{o,r^*} = 10^3$, the flow merges (i.e., the boundary layer completely fills the nozzle) at a point where $\delta/r^* \approx 3$. For these conditions, $\delta^*/\delta \sim 0(1/10)$. The ratio δ^*/δ tends to increase with wall temperature.

In general, the wall temperature seems to have a stronger effect on δ^* than on δ (Ref. 4). In Figs. 5, 7, and 8 the effect of nozzle wall temperature was investigated, with other conditions held constant, by considering $T_w/T_o = 1/10$, $T_w/T_o = 1/3$, and an adiabatic wall. For $Re_{o,r^*} = 10^4$, the ratio δ^*/δ at the nozzle exit was 0.30, 0.48, and 0.68, respectively.

The effect of Prandtl number was investigated by repeating the conditions of Fig. 5 but with Pr = 1 in place of 5/7. The results are presented in Fig. 9. The displacement thickness was found to increase for Pr = 1 by approximately 20 percent at the nozzle exit.

The conditions of Fig. 5 were also repeated using $\zeta = 1$ in place of $\zeta = 2/3$ to investigate the effect of the power law variation of vicosity with temperature. For $\zeta = 1$ the displacement thickness was found to decrease by 20 to 25 percent below that for $\zeta = 2/3$ (see Figs. 5 and 10). Note that, since $\bar{\mu} = \bar{T}^{\zeta}$ and $\bar{T} \leq 1$, then the flow is more viscous for $\zeta = 2/3$ than for $\zeta = 1$.

Velocity and temperature profiles calculated with and without transverse curvature terms are presented in Fig. 11 for Conditions 3 and 9 (Table I) with $Re_{o,r^*} = 3 \times 10^3$. Neglecting transverse curvature decreases the boundary-layer thickness for internal flow. The effect of transverse curvature is negligible for thin boundary layers, but may be significant for thick boundary layers. Further results and discussion concerning the effects of transverse curvature are reported in Ref. 5.

The displacement thicknesses of an axisymmetric and two-dimensional nozzle are presented in Fig. 12. For each nozzle, $A_e/A^* = 5$, and therefore, the two-dimensional nozzle is considerably longer since $\alpha = 10$ deg for each. The result is to produce a significantly larger displacement thickness for the two-dimensional nozzle than for the axisymmetric nozzle.

SECTION V
COMPARISONS WITH EXPERIMENTAL DATA AND OTHER THEORETICAL RESULTS

Curves of $Re_{o,r^*}/(p_o r^*)$ versus total temperature for various gases are presented in Fig. 13 for the convenience of determining Re_{o,r^*}. The viscosities used for all gases in Fig. 13 except carbon dioxide (CO_2) are those given by Svehla (Ref. 14). The viscosity of CO_2 was taken from Table 8.4-2 of Hirschfelder, Curtiss, and Bird (Ref. 15).

Highly viscous nozzle flows are usually associated with nozzles of small physical size. The spatial resolution of experimental measurements in such nozzles is obviously restricted. However, highly viscous flows can also be produced in large nozzles if sufficiently large volume flows can be pumped at low pressures, thereby permitting more detailed investigations of the boundary layer. Such investigations are possible in the Aerospace Research Chamber 10V in the VKF at AEDC. The present and some previous calculation methods will be compared with experimental data taken in Chamber 10V using a nominal Mach three nozzle, denoted M3 nozzle. This is a 10-deg half-angle conical nozzle with $d^* = 27$ cm, $d_e = 76.2$ cm, and $R = 11.2$ cm. The walls of this nozzle were cooled with liquid nitrogen to maintain a constant nozzle wall temperature of about 85°K.

Calculated and measured pitot pressure profiles at the nozzle throat are presented in Fig. 14. Nitrogen was the test gas used for these and all other experimental data presented in this report. The present results are in good agreement with the results using the method of Ref. 5. The calculated profiles are in relatively good agreement with the measured profile for these conditions.

Calculated and measured pitot pressure profiles at the nozzle exit are presented in Fig. 15. This calculation was performed using $\zeta = 2/3$, whereas some other results presented herein, e.g., Fig. 14, were obtained using Sutherland's viscosity law for nitrogen. However, over the temperature range of the experimental data taken in Chamber 10V, there was negligible difference in the results using either viscosity variation with temperature.

Present calculations are compared to calculations by the method of Rae (Ref. 10) and experimental data in Figs. 16 and 17. The present results are in relatively good agreement with the experimental data, but Rae's method is found to overestimate the size of the viscous region for these conditions. Results were also presented in Ref. 5 for the conditions of Fig. 17. The calculated profile from Ref. 5 is almost identical with the present result in Fig. 17 (see Ref. 5) and is not presented.

Pitot pressure profiles at about 7 throat radii downstream of the M3 nozzle throat are presented in Fig. 18 for $Re_{o,r^*} = 1170$. A relative minimum exists at the nozzle centerline in the experimentally measured profile, and slight "humps" or relative maximums exist near the edge of the boundary layer. It should be pointed out that the existence of humps does not necessarily imply that the flow is non-isentropic. Imagine a radial pitot pressure profile in an inviscid contoured supersonic nozzle which is sufficiently far downstream of the throat to pass through a portion of the uniform parallel flow near the centerline. Such a pitot profile would have lower values near the nozzle centerline than near the wall because of the larger Mach numbers near the centerline. However, the matching of such an inviscid flow with a realistic viscous flow requires the pitot pressure near the wall to approach the local static pressure which is less than the centerline pitot pressure. Therefore, it is not difficult to conceive of humps in such a radial pitot profile because of the matching of inviscid and viscous flow. This argument is based on flow in a contoured nozzle. It is applied to the present case because the displacement thickness effectively contours the nozzle. A more accurate approach of investigating such flows would be to remove the present assumption of one-dimensional inviscid flow outside the boundary layer and obtain more accurate solutions, such as, inviscid method-of-characteristics solutions. However, the pitot pressure profile is relatively well predicted in Fig. 18, and for this work, the assumption of one-dimensional inviscid flow outside the boundary layer is considered acceptable.

Just as radial pitot profiles with humps do not necessarily imply that the flow is non-isentropic, a flat radial profile does not necessarily imply that the flow is isentropic. Consider the pitot pressure data in Fig. 19. Both the calculated and measured profiles are relatively flat for y/r_w larger than about 0.7. However, in this case the pitot profile is not a good measure of the extent of the nozzle wall viscous effects as shown in Fig. 20. From Fig. 20, the boundary-layer thickness as estimated from the pitot profile is about 55 percent of the nozzle radius, whereas it is calculated to be actually over 80 percent. The pitot profile for the case in Fig. 20 implies that 20 percent of the cross-sectional area of the nozzle at this point is core flow, whereas actually less than 4 percent is core flow. The reason a pitot profile might lead one astray is associated with the temperature or thermal boundary layer since pitot pressure depends, among other things, on $u/(T)^{1/2}$. The velocity variation is usually well behaved and fairly accurately predicted by simple analytical expressions based on boundary-layer thickness (Ref. 4); however, this is not the case with the thermal boundary layer. The temperature variation depends not only on local wall and edge values and gradients but also on the upstream conditions.

Therefore, some consideration should be given to the temperature variation in order to place limits-of-confidence on the use of pitot pressure as an indication of the nozzle wall viscous effects.

Carden (Ref. 16) measured local heat-transfer coefficients in an axisymmetric nozzle for $Re_{o,r^*} = 5 \times 10^3$. The experimental data were compared with calculated heat-transfer coefficients in Refs. 5 and 16. However, Whitfield made a mistake in Ref. 5 and presented solutions for $r^* = 0.262$ cm instead of $d^* = 0.262$ cm (0.103 in.) which corresponds to the actual nozzle throat dimension. Because of this error, the calculated heat-transfer coefficients (Ref. 5) from the iterated solutions were significantly below the experimental data of Carden (Ref. 16). Heat-transfer coefficients were calculated using the present method but with the inappropriate throat dimension of $r^* = 0.262$ cm, and good agreement was obtained with the calculated results of Ref. 5. Results were also obtained with the present method using the proper throat dimension of $d^* = 0.262$ cm, and good agreement with the experimental data was obtained as shown in Fig. 21. Also, in Fig. 21 are results from two of the methods Carden (Ref. 16) used for calculating the heat-transfer coefficient and one solution from Ref. 5. Although the result from Ref. 5 which is presented in Fig. 21 was not iterated to include the higher-order displacement effect, the result was obtained using the pressure distribution corresponding to the proper nozzle geometry and, therefore, is included in Fig. 21. This result from Ref. 5 is in relatively good agreement with the present result. All calculation methods underestimate the most upstream uncorrected experimental data point in Fig. 21. However, Carden points out that radiation from the arc used to heat the gas could increase the total heat-transfer rate to this portion of the nozzle. No corrections for radiation heat transfer were made to the experimental data.

It might be pointed out that the heat-transfer rate printed out in the present program, denoted as AJI(1), is equal to $q_w/(\rho_o H_o^{3/2})$. Although made dimensionless, the numerical scheme used in Ref. 11 to calculate AJI(1) is retained in the present code in subroutine WALL.

SECTION VI
CONCLUSIONS

The present results were shown to be in good agreement with results from the method of Ref. 5. Although it was noted during the present investigation that more axial stations were required using the present program than that of Ref. 5 to obtain the same degree of accuracy (presumably this is due to the transformation variables used in Ref. 5, which are advantageous for thin boundary layers but disadvantageous for thick internal boundary layers), the present program is much smaller, faster and easier to use. Comparisons with results from Rae's method (Ref. 10) and experimental data indicated the present method to be more accurate than Rae's for the conditions considered. It should be remembered, however, that the present work is not applicable to merged flows without modification, whereas Rae's method is more applicable to merged flows.

Consistent agreement was obtained between the present results and experimental data. Except for the heat-transfer data, the experimental data were taken in a relatively large nozzle where the boundary layer could be accurately probed. Similar agreement was obtained in Ref. 2 where extensive data were obtained in small nozzles, $r^* \sim 0$ (0.1 cm). The numerical method used in Ref. 2 was developed by Mayne (Ref. 2), as stated previously, and differs from the original Patankar and Spalding method (Ref. 11) primarily in the numerical scheme near the wall.

The present method has not been modified for use in nozzle design; however, it is a straightforward matter to make such a modification (see Ref. 5). To design a nozzle, a new nozzle geometry, $r_w(x)$, is calculated from the displacement thickness from each iteration, and the new geometry is used for the next iteration while the desired axial pressure distribution is maintained for each iteration. It was found in Ref. 5 that convergence was, in general, more rapid in iterating on the nozzle geometry than on the axial pressure distribution.

REFERENCES

1. Smithson, H. K., Price, L. L. and Whitfield, D. L. "Wind Tunnel Testing of Interactions of High Altitude Rocket Plumes with the Free Stream." AEDC-TR-71-118 (AD731141), September 1971.

2. Whitfield, D. L., Lewis, J. W. L., Williams, W. D., et. al. "Specie Number Density, Pitot Pressure, and Flow Visualization in the Near Field of Two Supersonic Nozzle Banks Used for Chemical Laser Systems." AEDC-TR-73-11, May 1973.

3. Potter, J. L. and Carden, W. H. "Design of Axisymmetric Contoured Nozzles for Laminar Hypersonic Flow." Journal of Spacecraft and Rockets, Vol. 5, No. 9, September 1968, pp. 1095-1100.

4. Whitfield, D. L. "Theoretical and Experimental Investigation of Boundary Layers in Low-Density Hypersonic Axisymmetric Nozzles." AEDC-TR-68-193 (AD674597), September 1968.

5. Whitfield, D. L. and Lewis, C. H. "Boundary-Layer Analysis of Low-Density Nozzles, Including Displacement, Slip, and Transverse Curvature." Journal of Spacecraft and Rockets, Vol. 7, No. 4, April 1970, pp. 462-468.

6. Cohen, C. B. and Reshotko, E. "Similar Solutions for the Compressible Laminar Boundary Layer with Heat Transfer and Pressure Gradient." NACA Report 1293, 1956.

7. Jaffe, N. A., Lind, R. C., and Smith, A. M. O. "Solution to the Binary Diffusion Laminary Boundary Layer Equations Including the Effect of Second-Order Transverse Curvature." AIAA Journal, Vol. 5, No. 9, September 1967, pp. 1563-1569.

8. Adams, J. C., Jr. "Similar Solutions for Viscous Compressible Laminar Flow in Slender Axisymmetric Channels." Ph. D. Dissertation, North Carolina State University, 1966.

9. Williams, J. C., III. "Conical Nozzle Flow with Velocity Slip and Temperature Jump." AIAA Journal, Vol. 5, No. 12, December 1967, pp. 2128-2134.

10. Rae, W. J. "Some Numerical Results on Viscous Low-Density Nozzle Flows in the Slender-Channel Approximation." AIAA Journal, Vol. 9, No. 5, May 1971, pp. 811-820.

11. Patankar, S. V. and Spalding, D. B. Heat and Mass Transfer in Boundary Layers. Morgan-Grampian: London 1967.

12. Probstein, R. F. and Elliott, E. "The Transverse Curvature Effect in Compressible Axially Symmetric Laminar Boundary-Layer Flow." Journal of the Aeronautical Sciences, Vol. 23, No. 3, 1956, pp. 208-222.

13. Smith, G. D. Numerical Solution of Partial Differential Equations. Oxford University Press, New York, 1965.

14. Svehla, R. A. "Estimated Viscosities and Thermal Conductivities of Gases at High Temperatures." NASA TR-R-132, Washington, 1962.

15. Hirschfelder, J. O., Curtiss, C. F., and Bird, R. B. Molecular Theory of Gases and Liquids. John Wiley & Sons, Inc., New York, 1954.

16. Carden, W. H. "Local Heat-Transfer Coefficients in a Nozzle with High-Speed Laminar Flow." AIAA Journal, Vol. 3, No. 12, December 1965, pp. 2183-2188.

17. Beckwith, I. E. and Cohen, N. B. "Application of Similar Solutions to Calculation of Laminar Heat Transfer on Bodies with Yaw and Large Pressure Gradient in High-Speed Flow." NASA TND-625, 1961.

18. Pasqua, P. F., Stevens, P. N., Mott, J. E., Roland, H. C., and Robinson, J. C. "Analytical Studies on Nozzle Throat Cooling." AEDC-TDR-63-58 (AD400746), 1963.

APPENDIXES

I. ILLUSTRATIONS
II. TABLE
III. BOUNDARY-LAYER COMPUTER CODE
IV. INITIAL PRESSURE DISTRIBUTION COMPUTER CODE

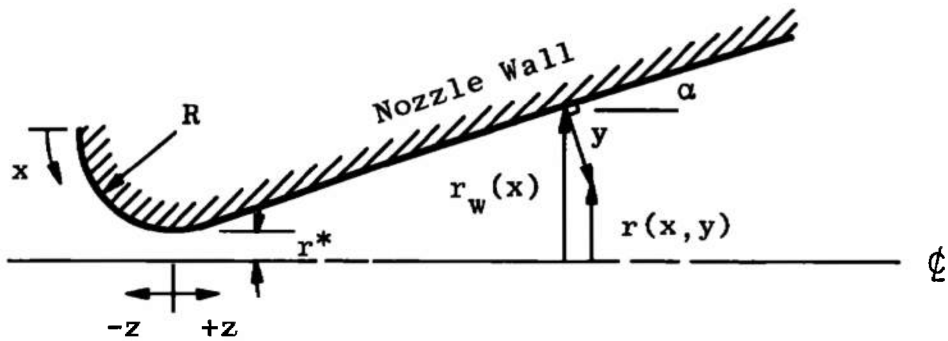

Fig. 1 Definition of Coordinate System

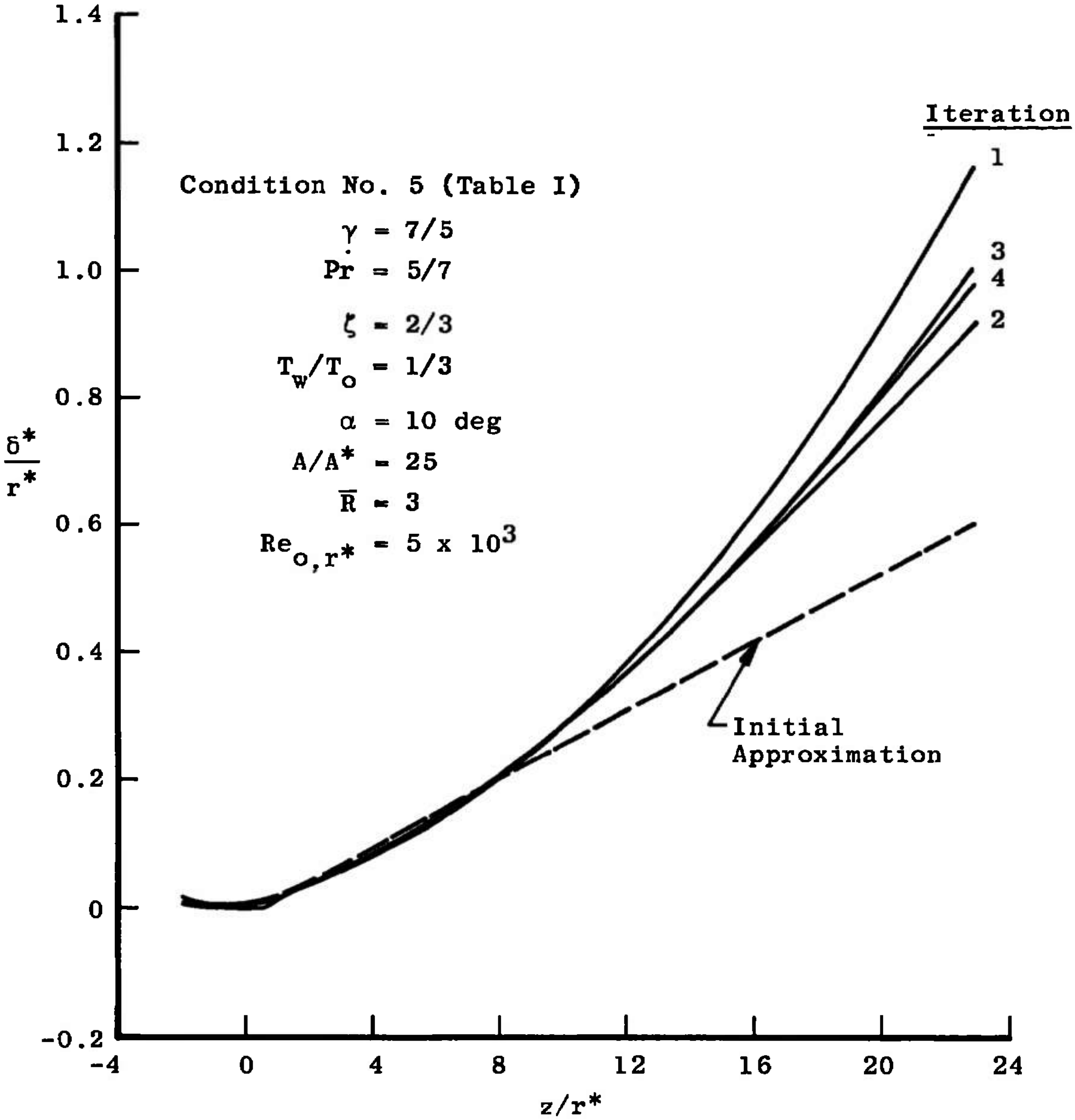

Fig. 2 Displacement Thickness of Successive Iterations for Condition No. 5 (Table I)

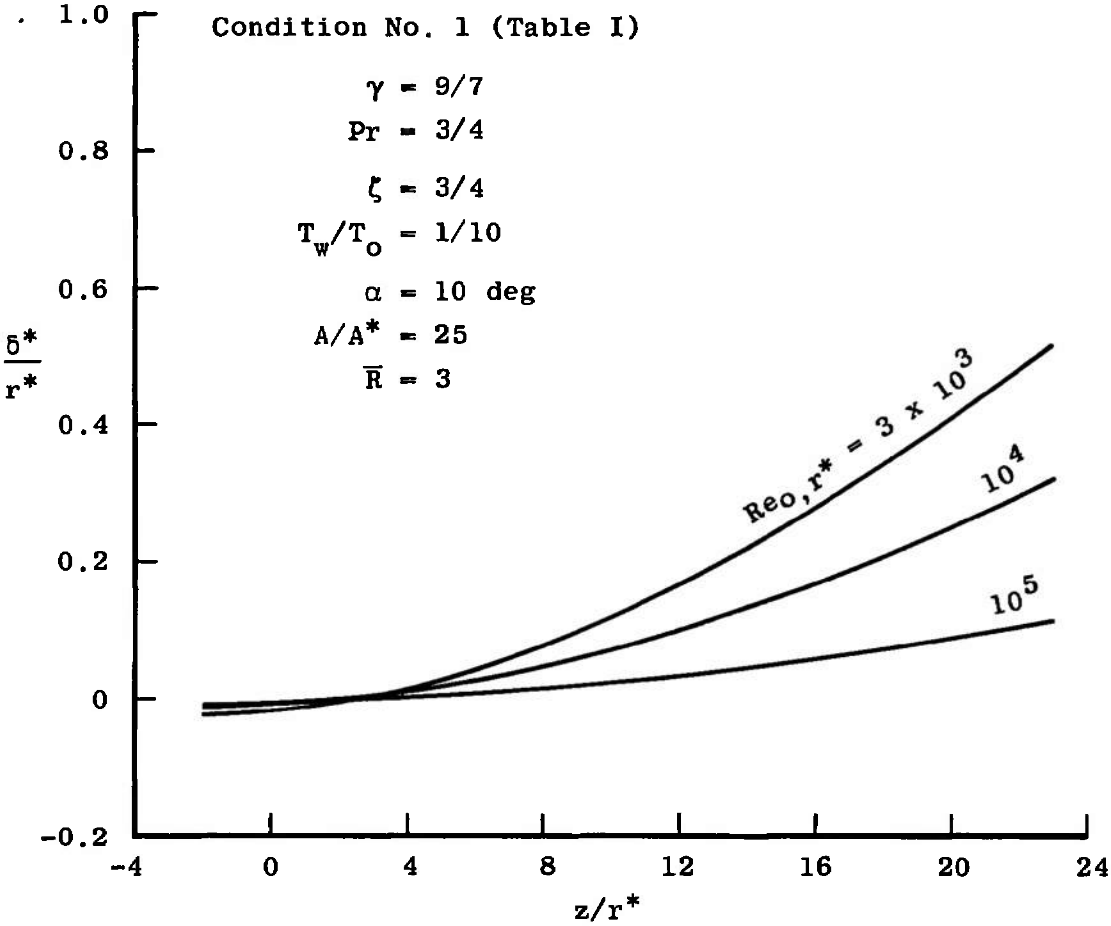

Fig. 3 Displacement Thickness for Condition No 1 (Table I)

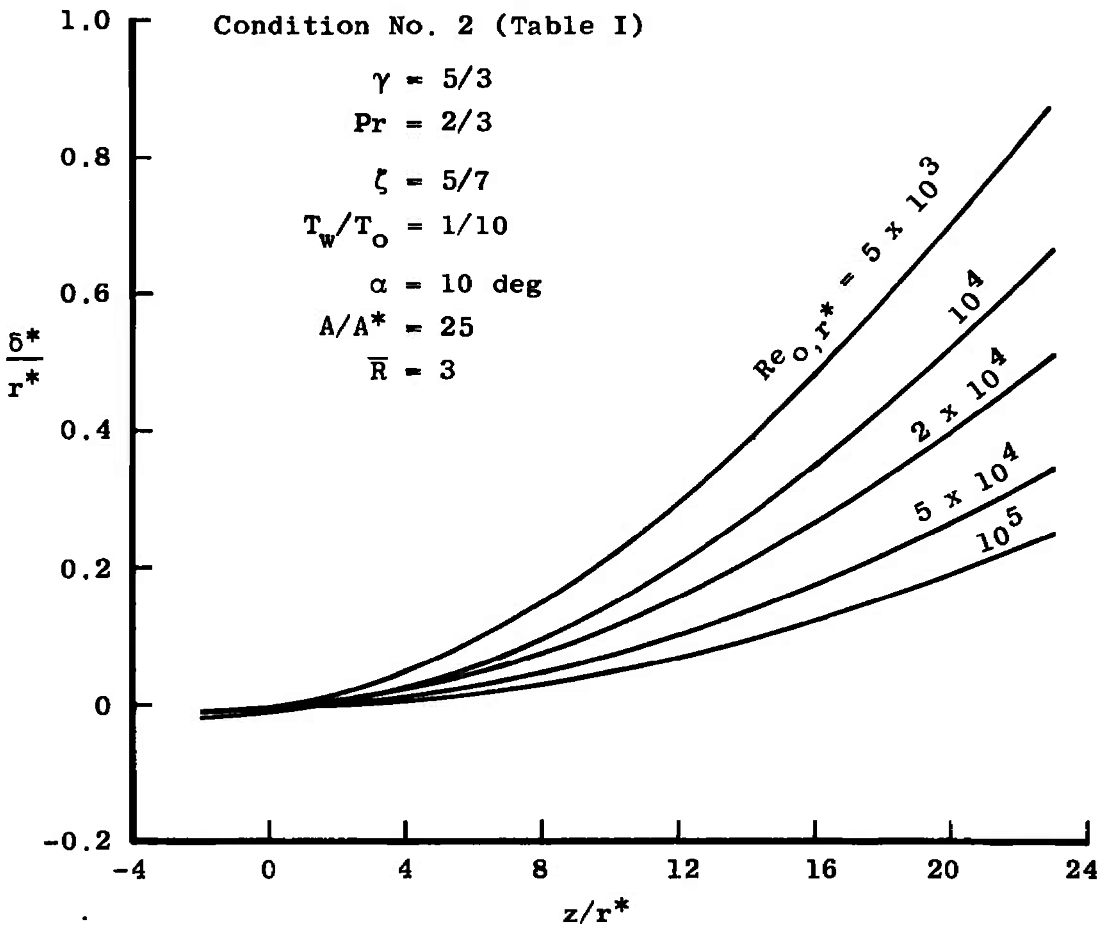

Fig. 4 Displacement Thickness for Condition No. 2 (Table I)

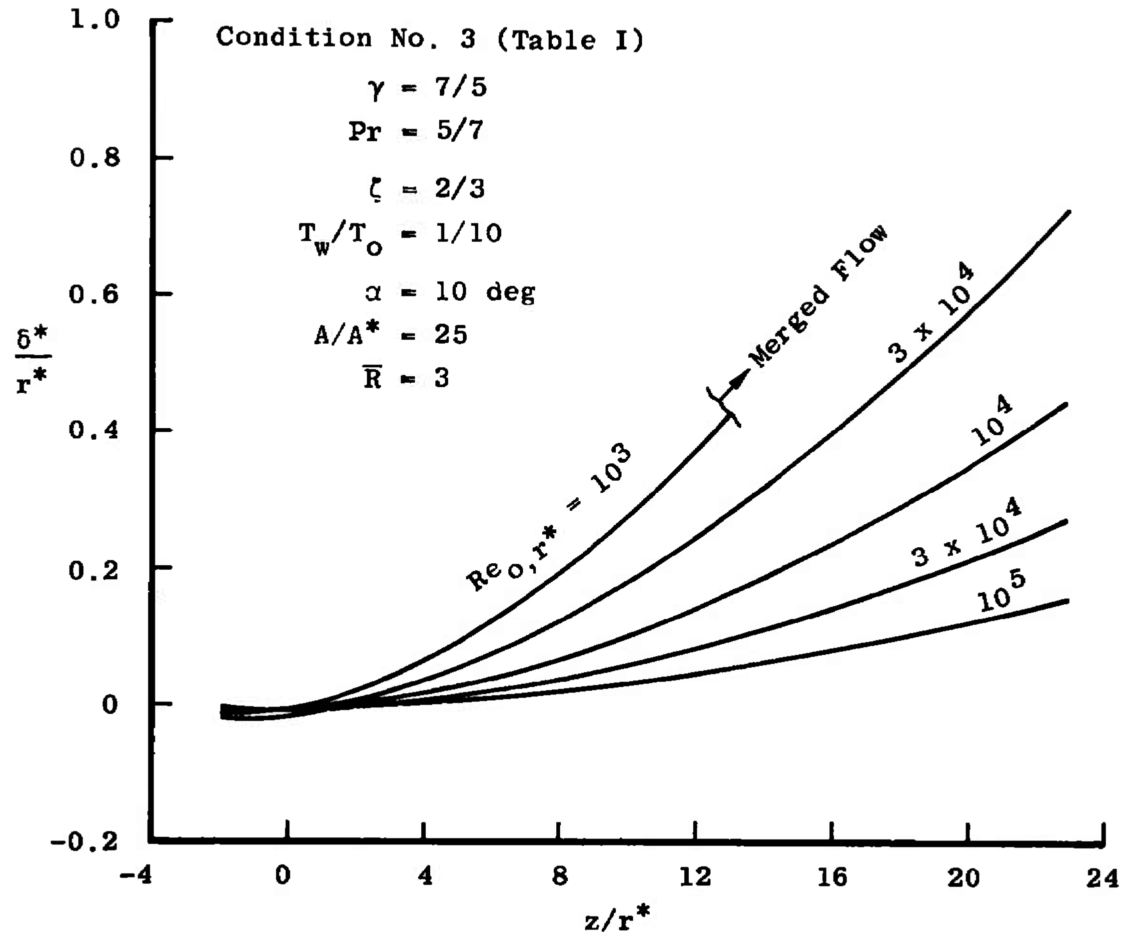

Fig. 5 Displacement Thickness for Condition No. 3 (Table I)

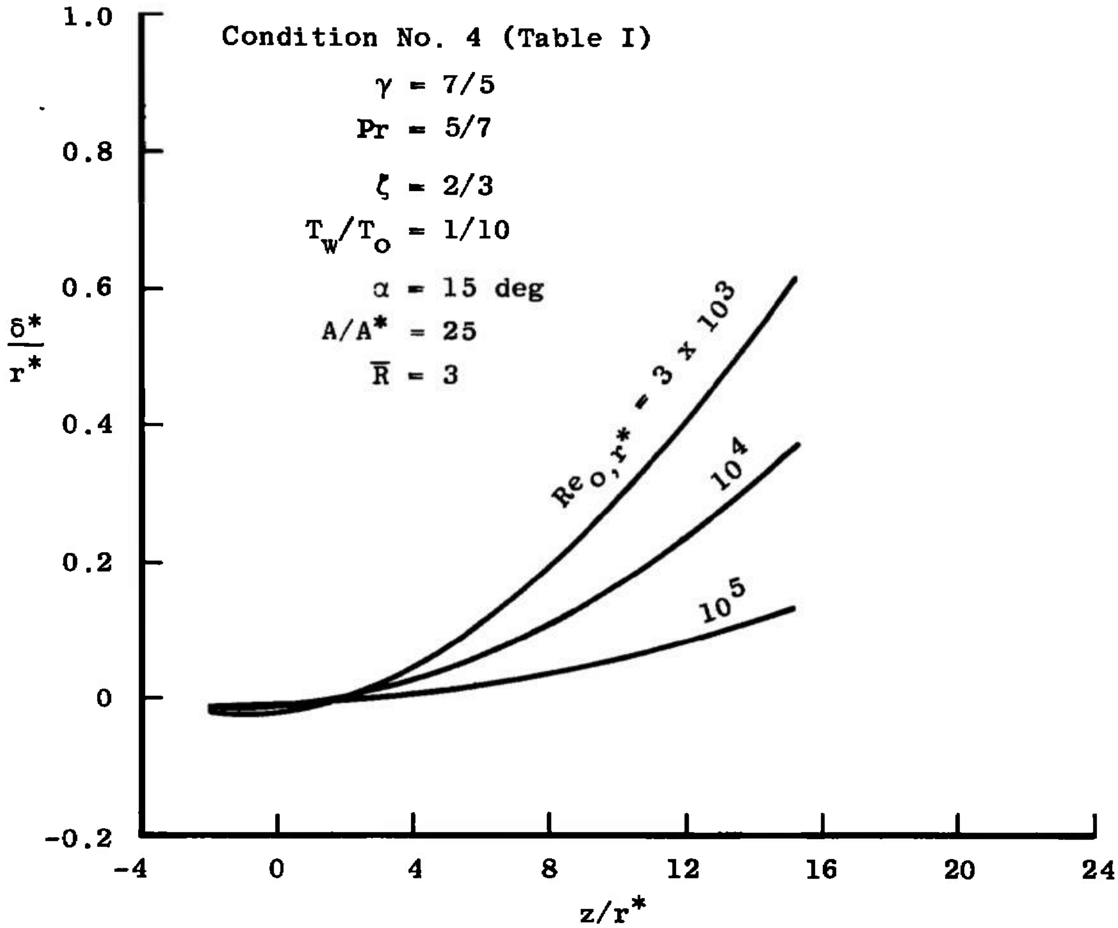

Fig. 6 Displacement Thickness for Condition No. 4 (Table I)

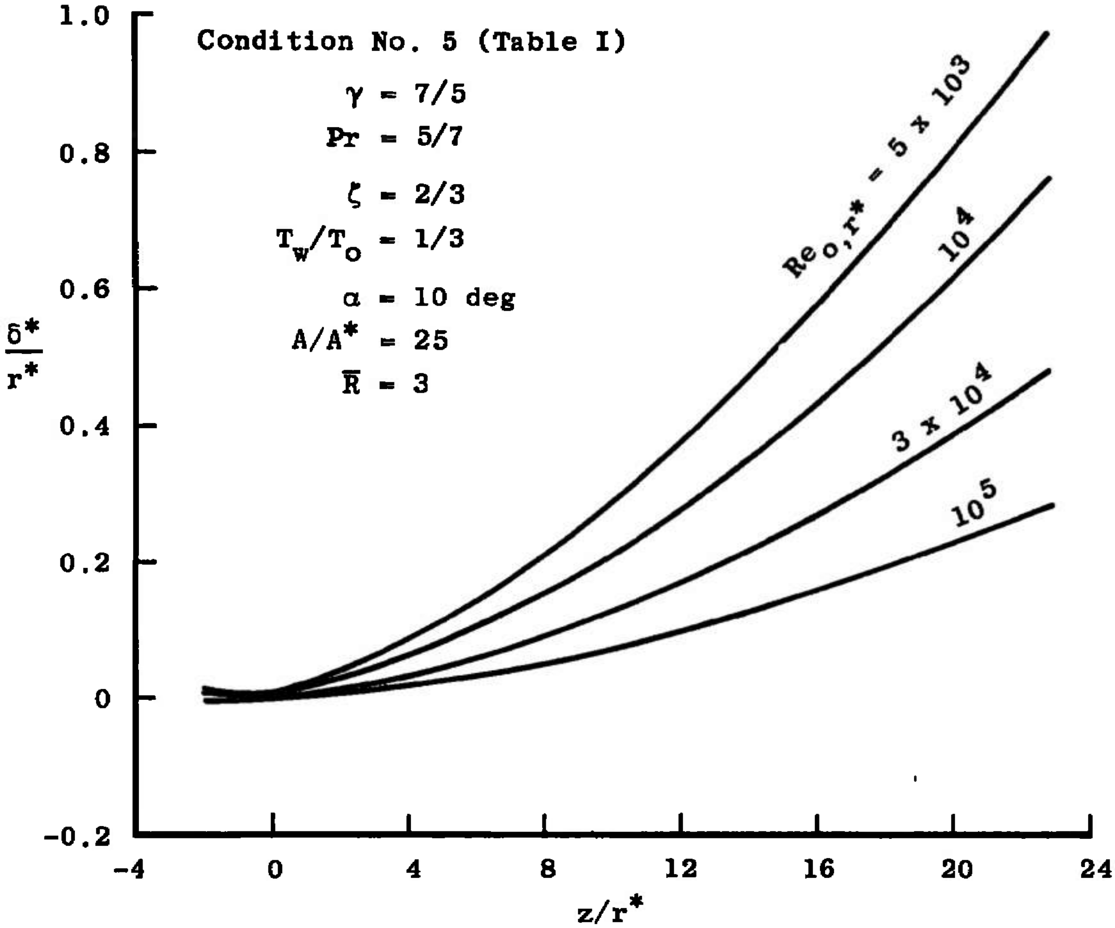

Fig. 7 Displacement Thickness for Condition No. 5 (Table I)

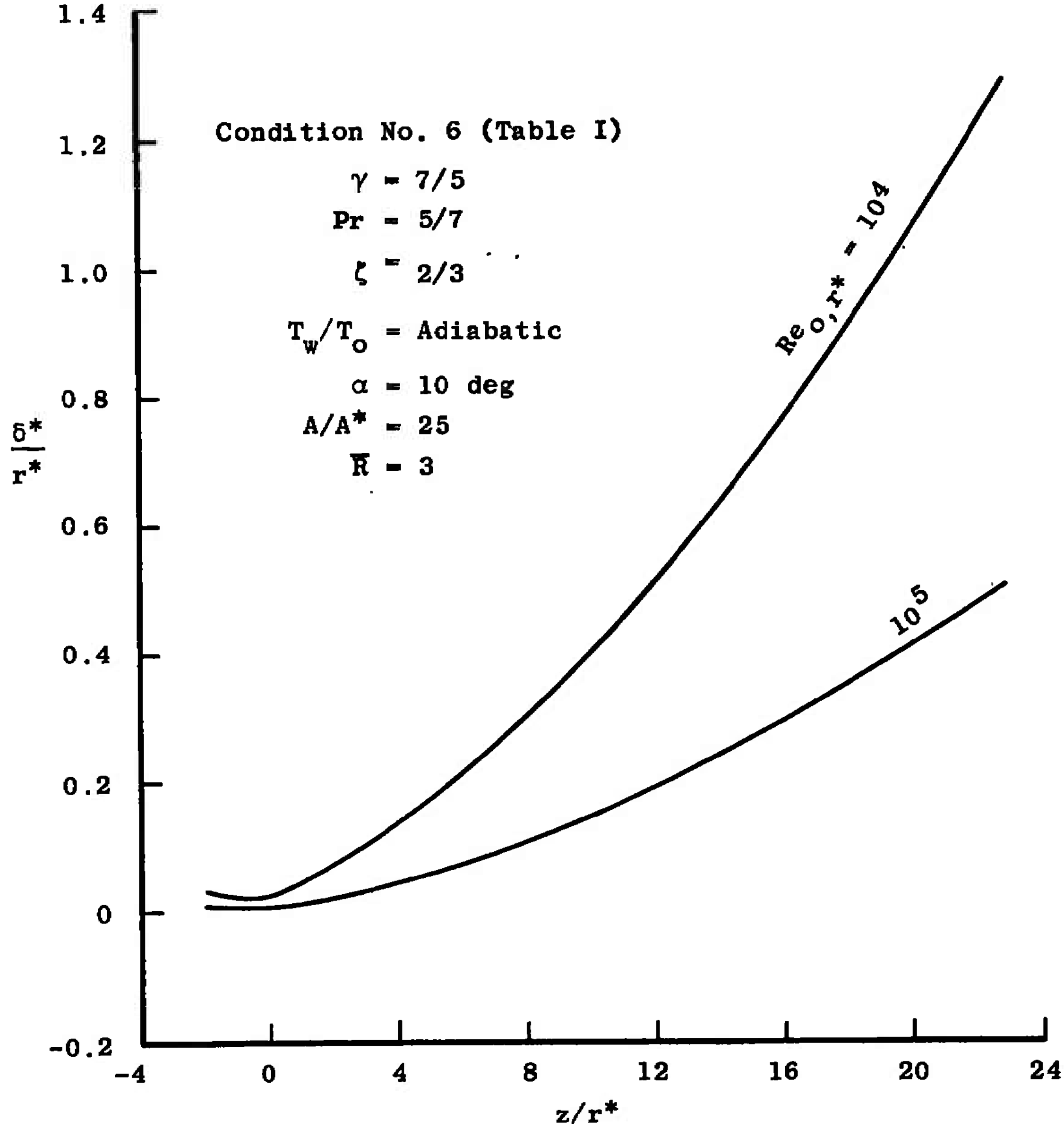

Fig. 8 Displacement Thickness for Condition No. 6 (Table I)

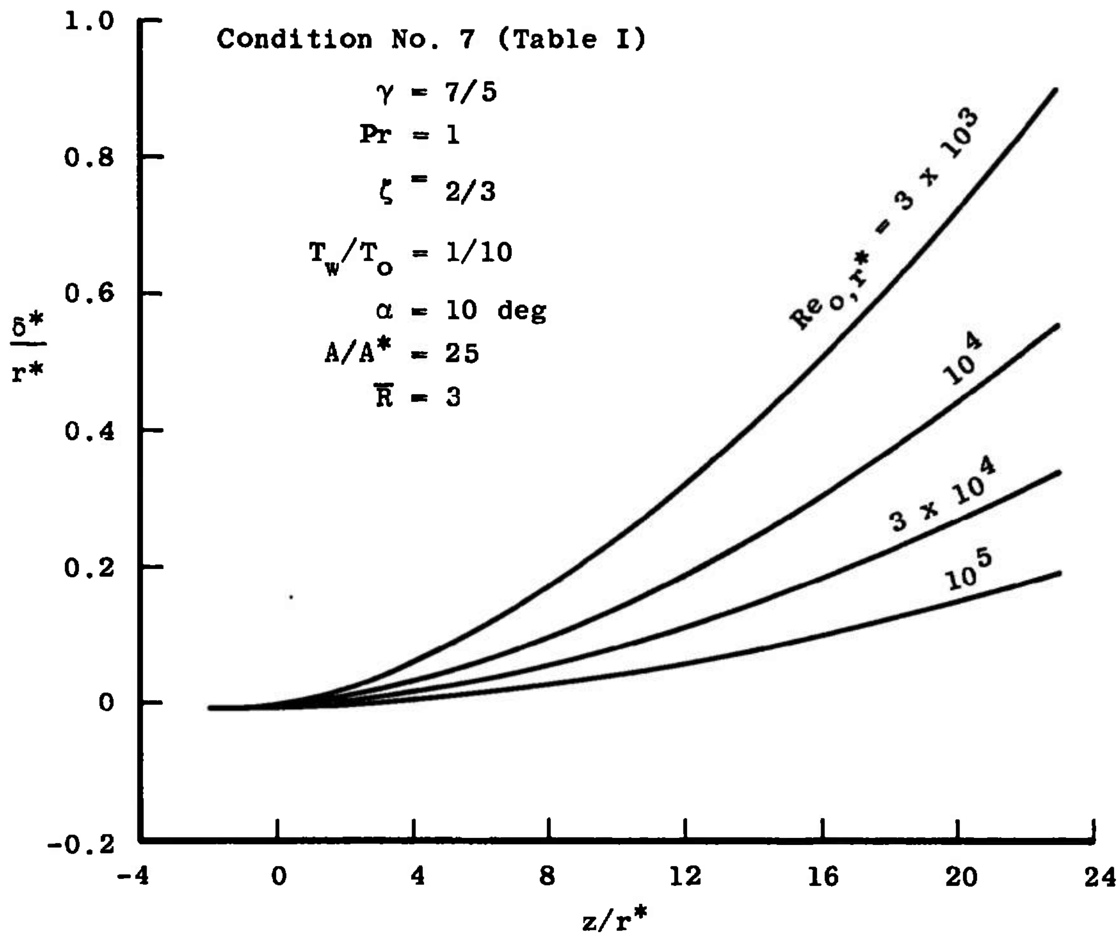

Fig. 9 Displacement Thickness for Condition No. 7 (Table I)

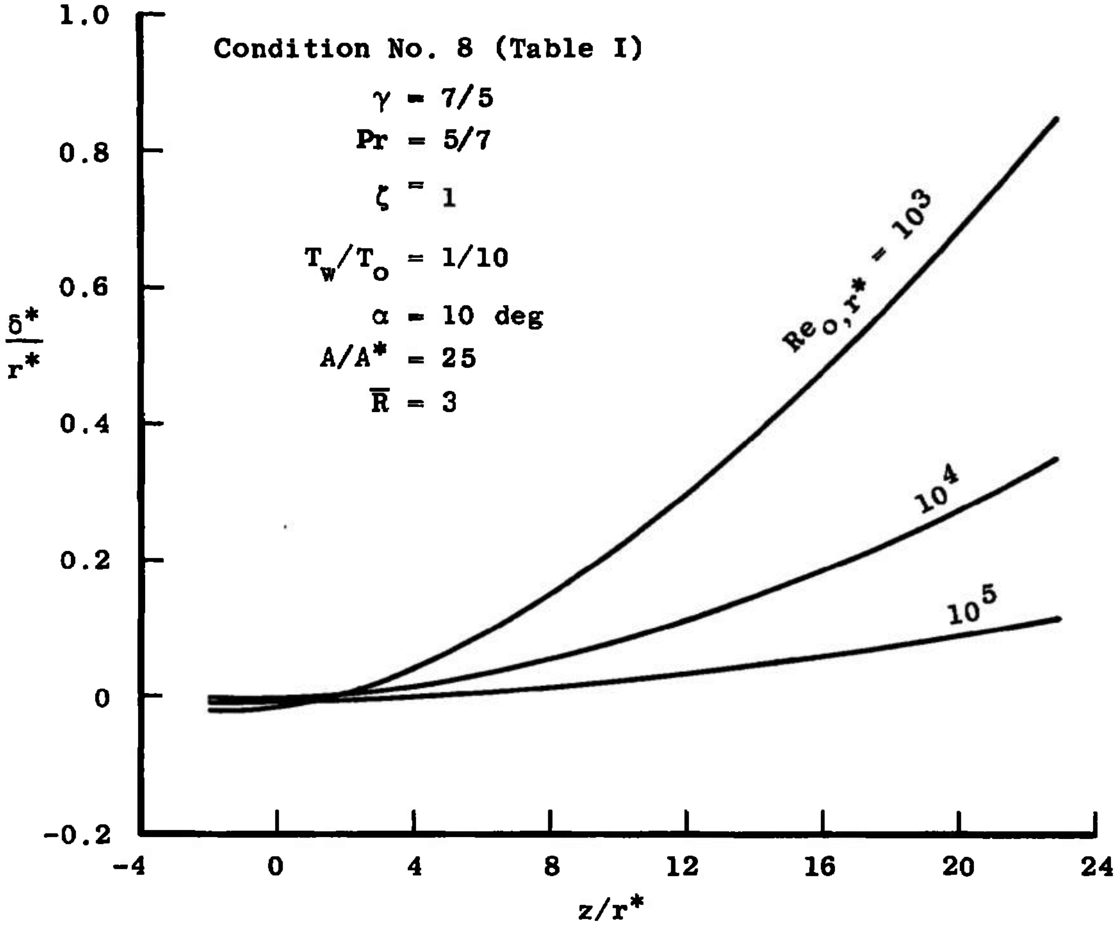

Fig. 10 Displacement Thickness for Condition No. 8 (Table I)

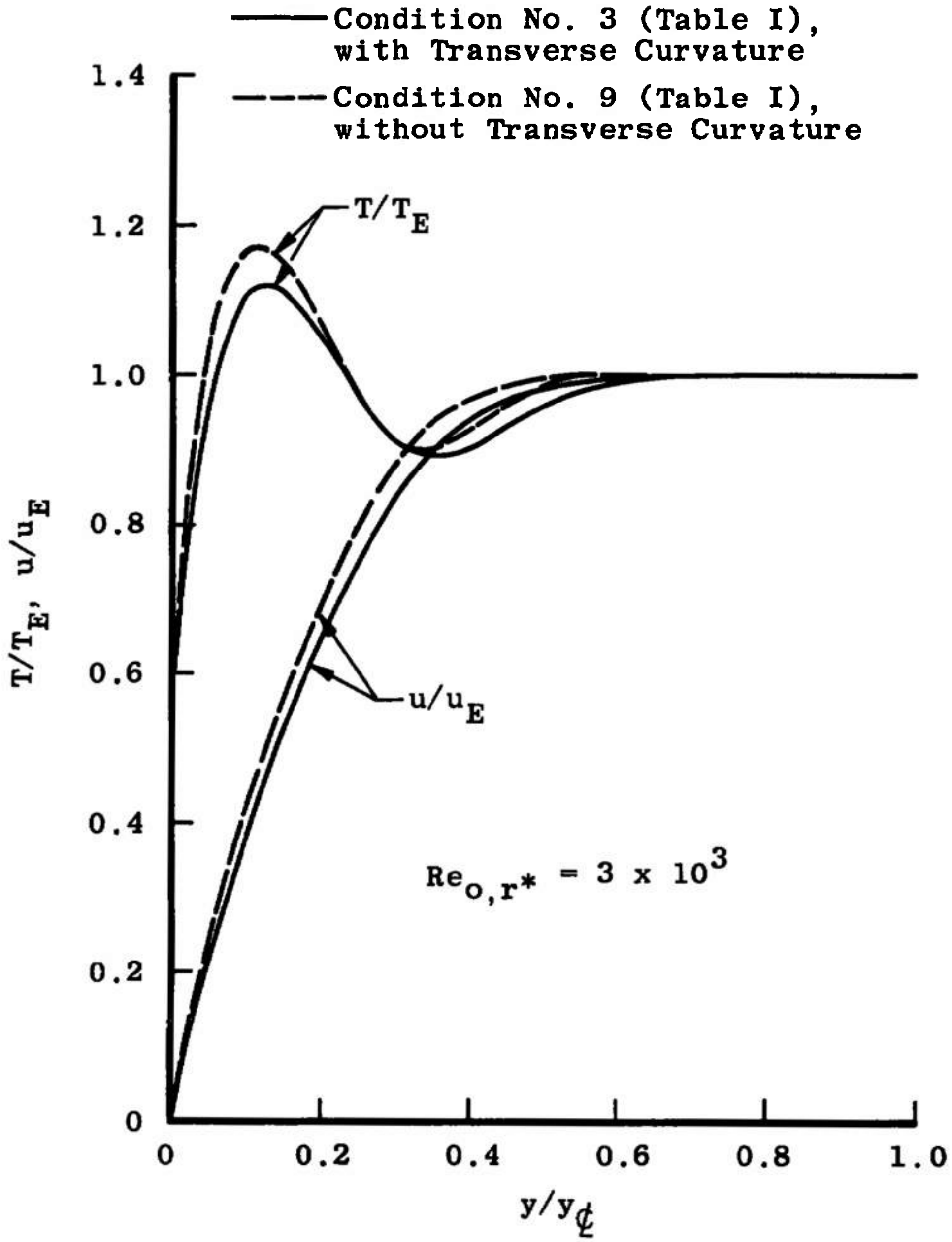

Fig. 11 Nozzle Exit Velocity and Temperature Profiles for Condition Nos. 3 and 9 (Table I)

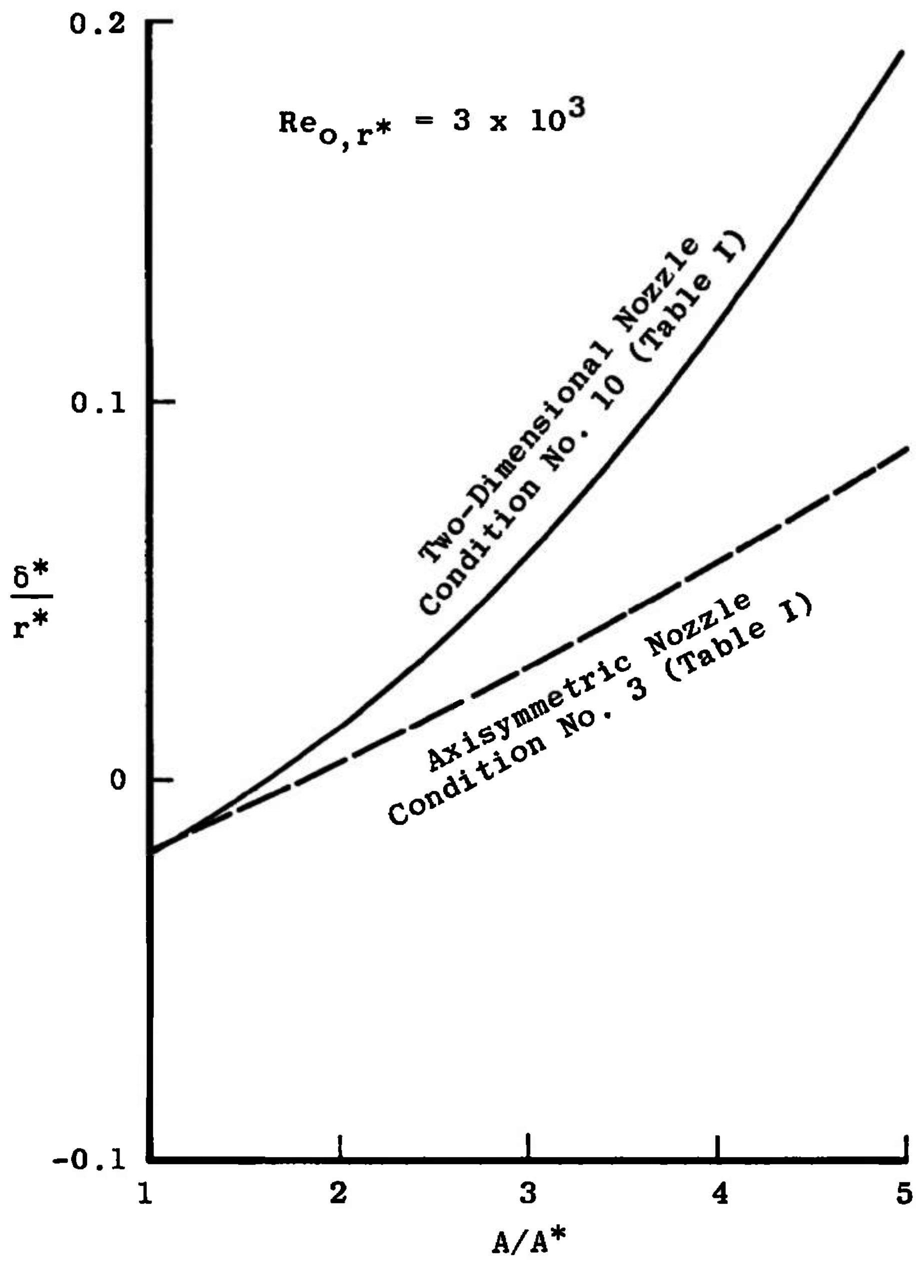

Fig. 12 Displacement Thicknesses of an Axisymmetric and Two-Dimensional Nozzle with Equal Area Ratios

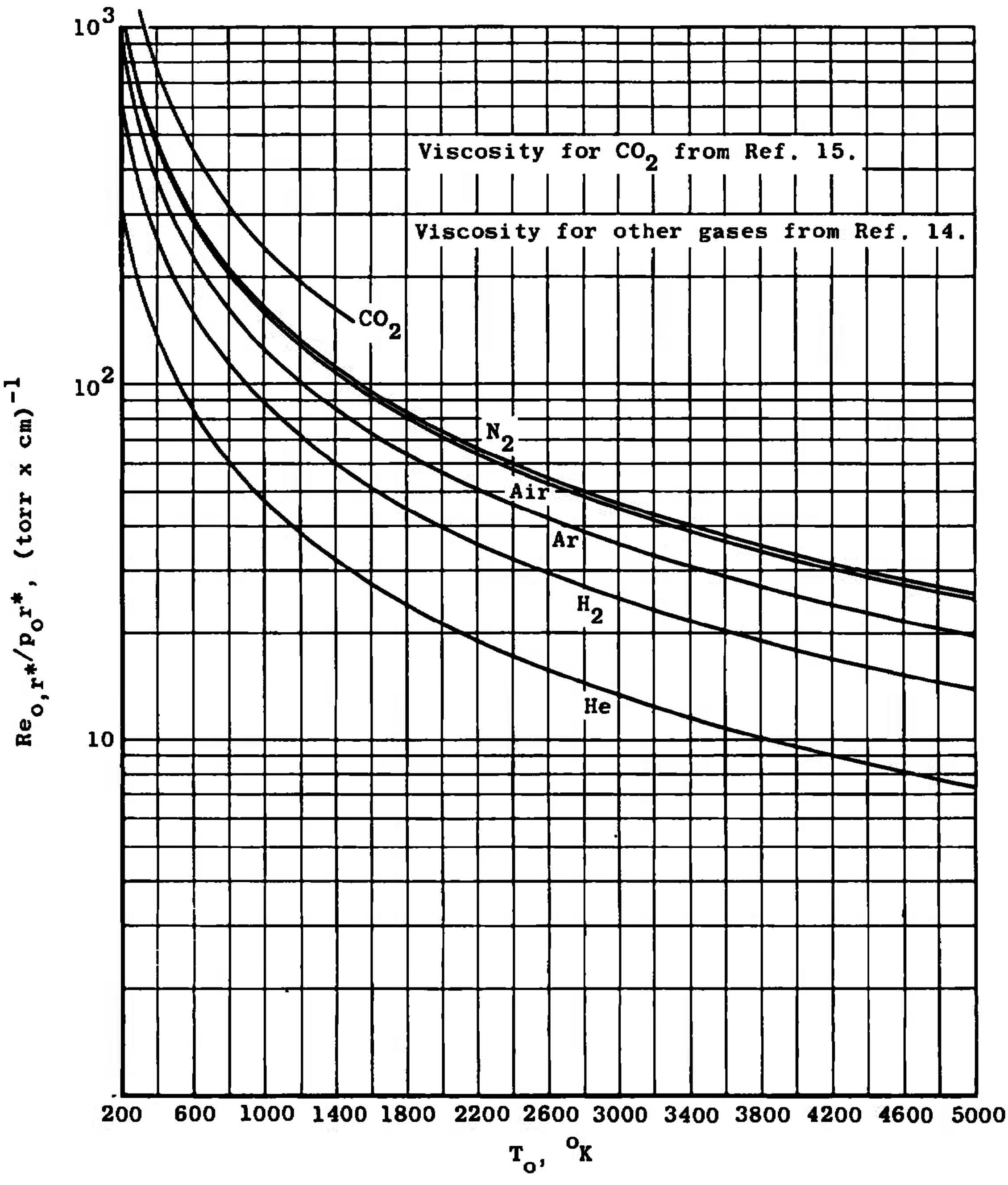

Fig. 13 Reservoir Reynolds Number as a Function of p_o, T_o, and r^* for Various Gases

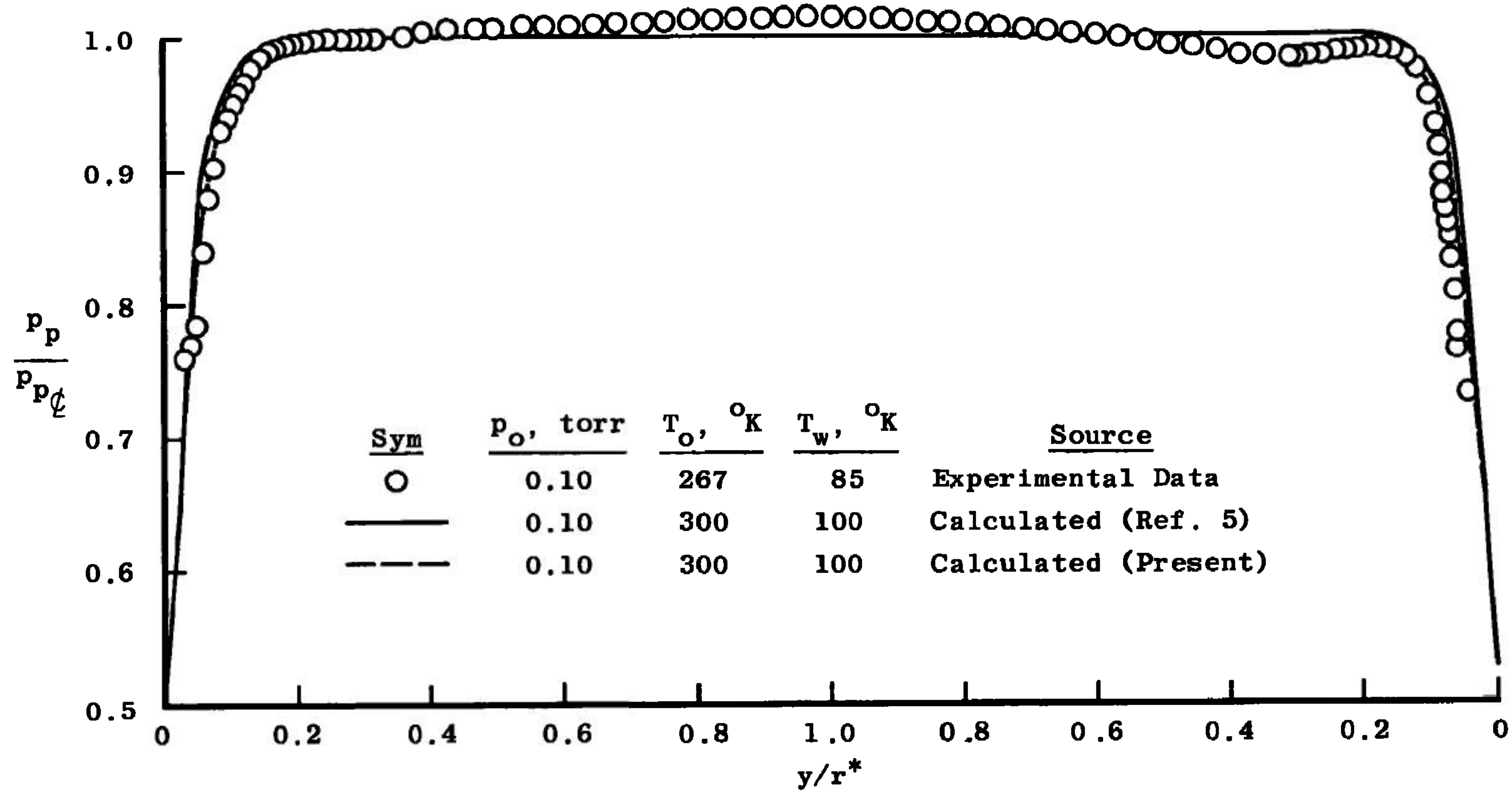

Fig. 14 Calculated and Measured Pitot Pressure Profiles at the M3 Nozzle Throat for Re_{o,r^*} = 900

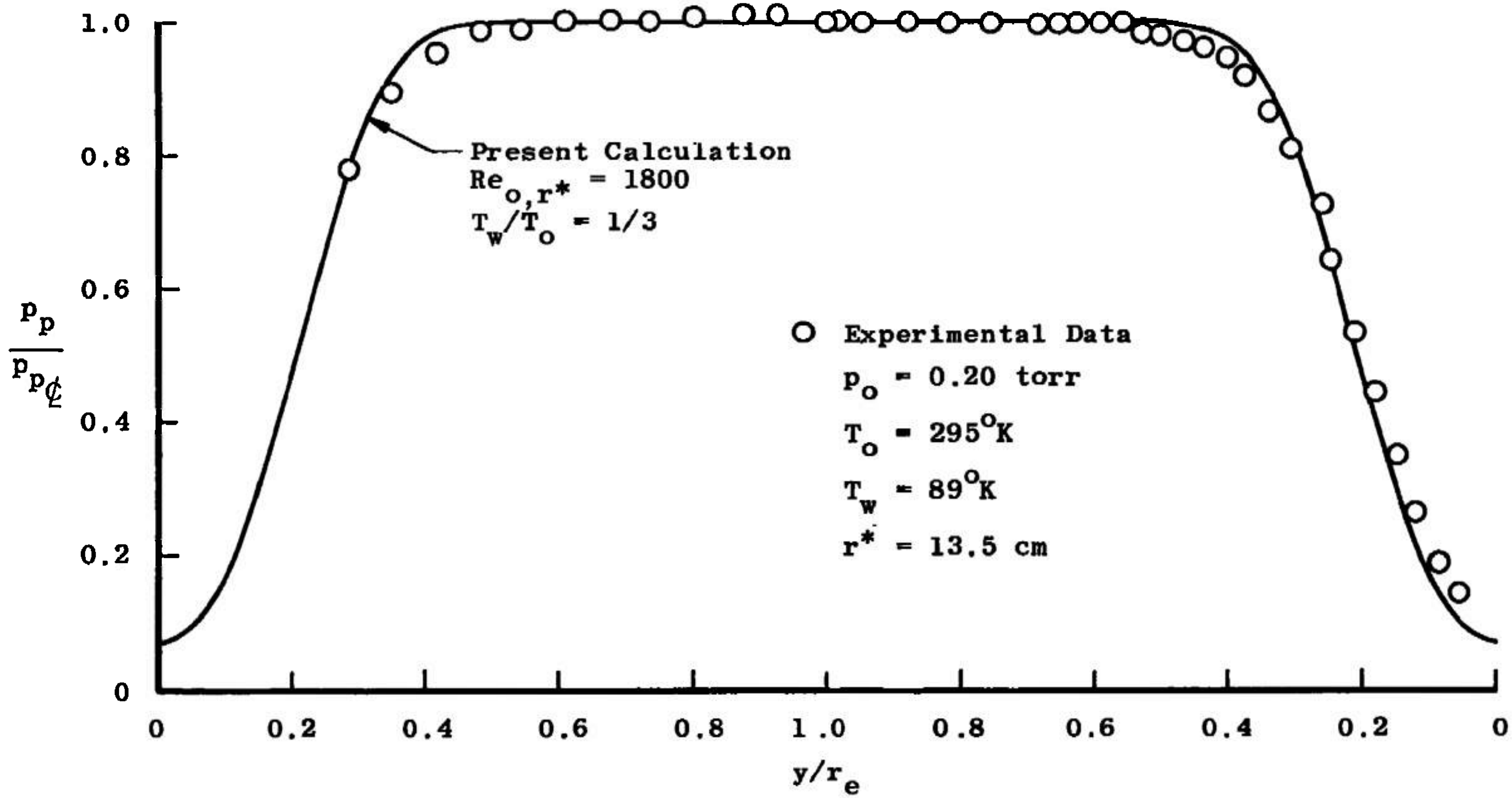

Fig. 15 Calculated and Measured Pitot Pressure Profiles at the M3 Nozzle Exit for Re_{o,r^*} = 1800

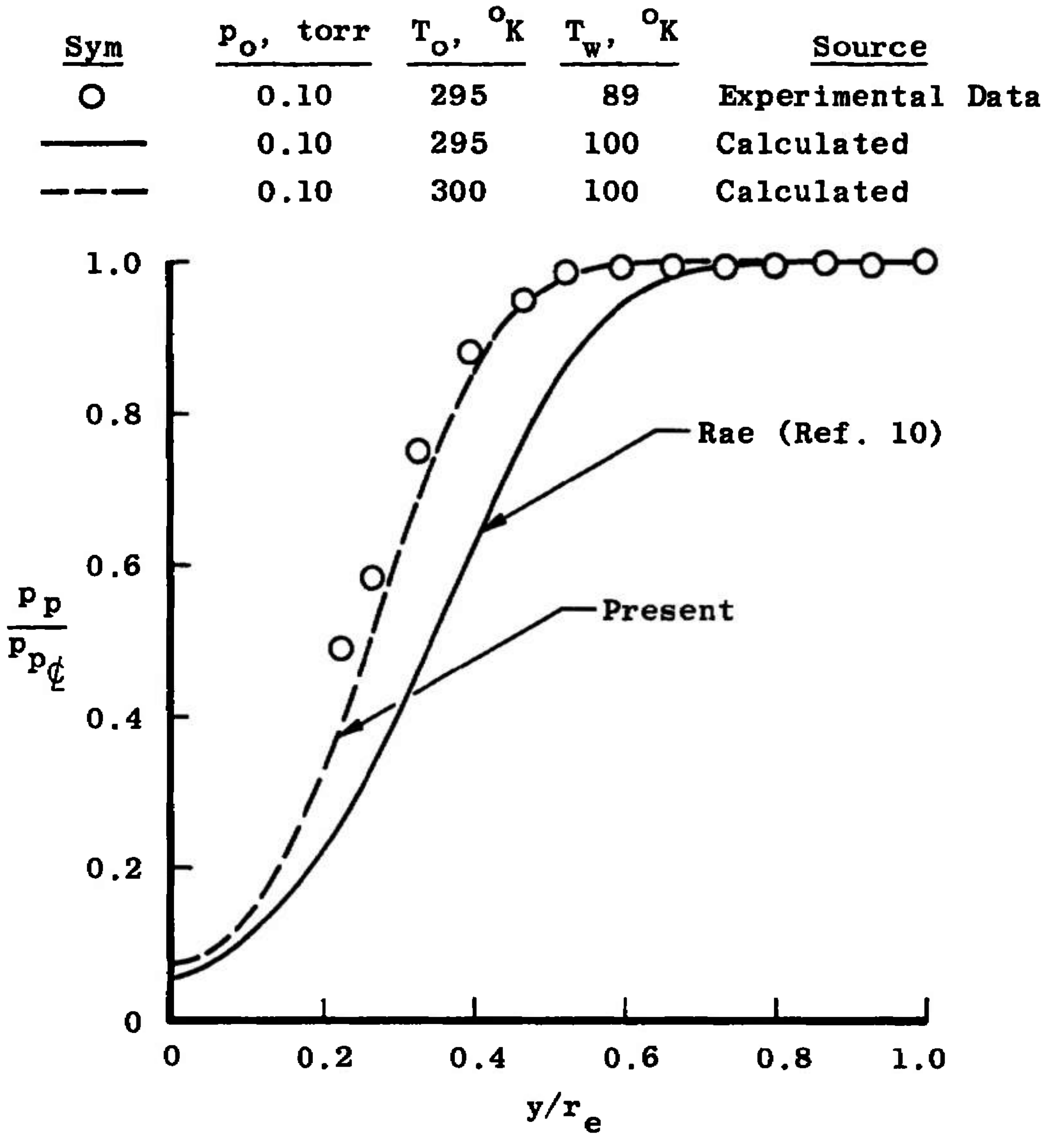

Fig. 16 Calculated and Measured Pitot Pressure Profiles at the M3 Nozzle Exit for Re_{o,r^*} = 900

Sym	p_o, torr	T_o, °K	T_w, °K	Source
○	0.50	280	89	Experimental Data
———	0.50	300	100	Calculated
— —	0.50	300	89	Calculated

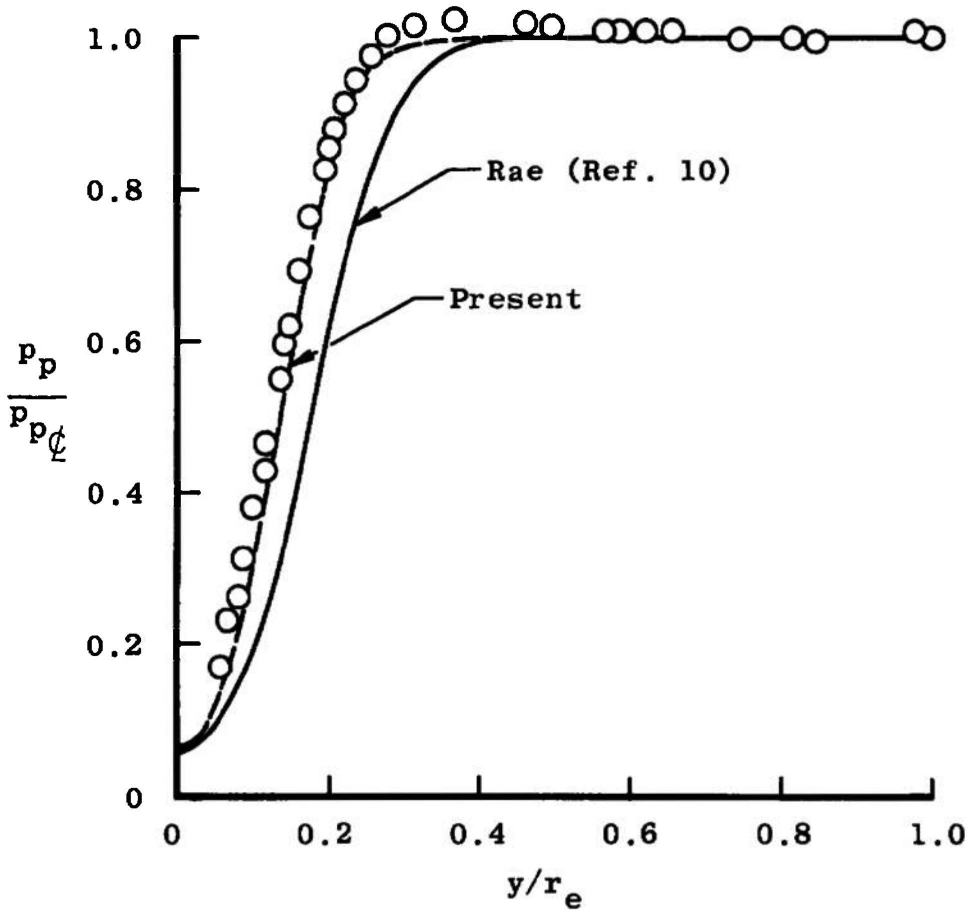

Fig. 17 Calculated and Measured Pitot Pressure Profiles at the M3 Nozzle Exit for $Re_{o,r*}$ = 4500

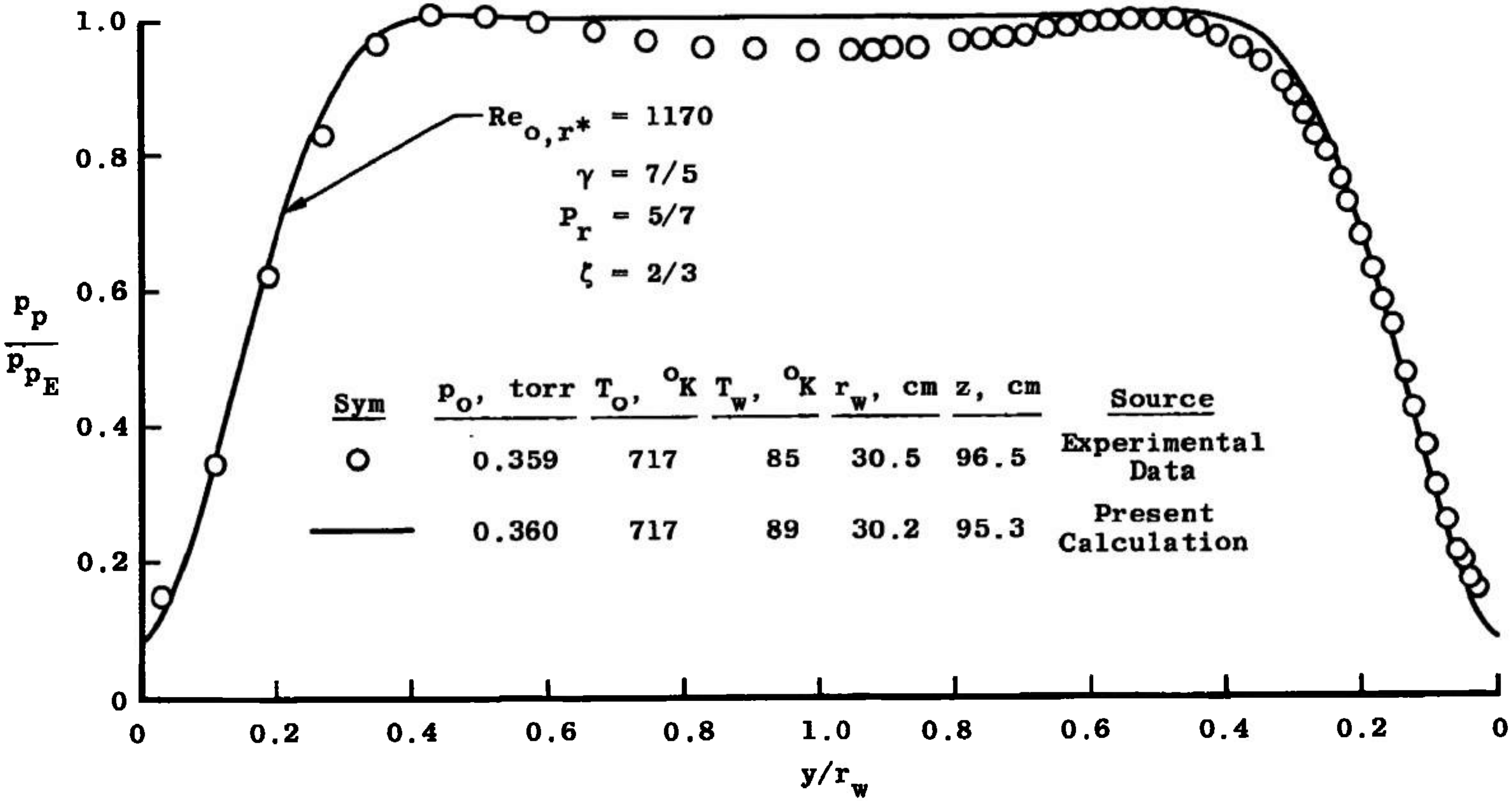

Fig. 18 Calculated and Measured Pitot Pressure Profiles Downstream of the M3 Nozzle Throat for Re_{o,r^*} = 1170

Sym	p_o, torr	T_o, °K	T_w, °K	v_w, cm	z, cm	Source
O	0.103	717	85	30.5	96.5	Experimental Data
———	0.100	717	89	29.0	88.6	Present Calculation

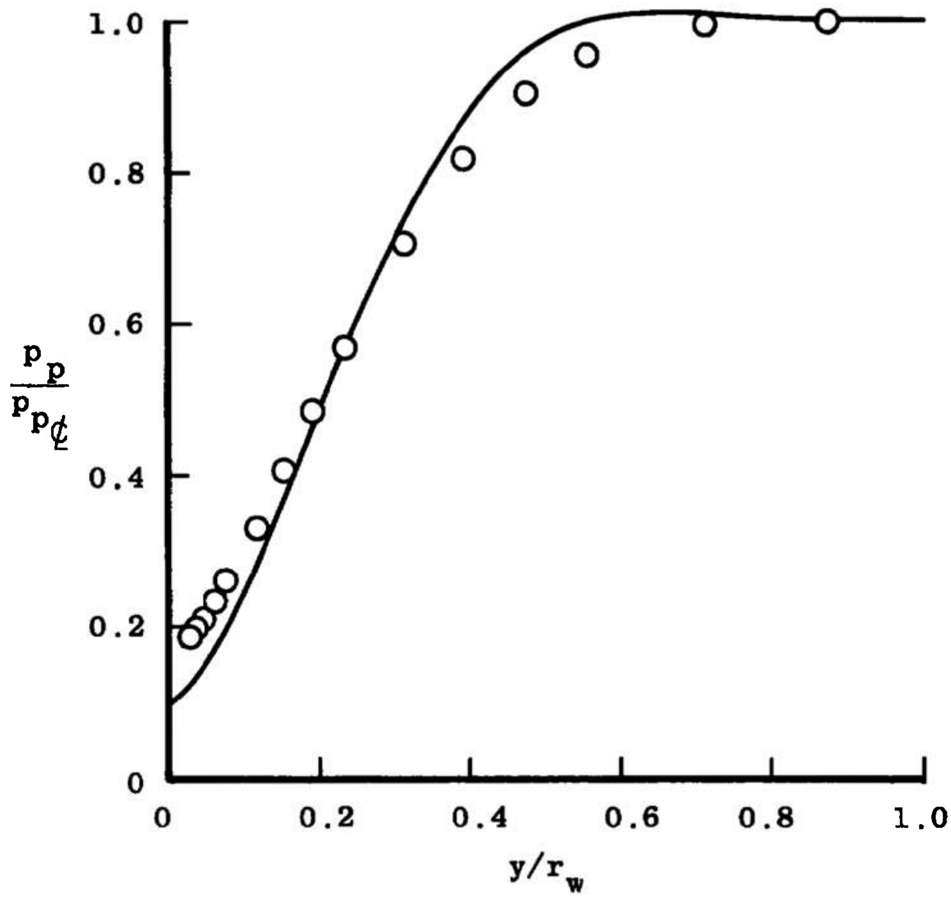

Fig. 19 Calculated and Measured Pitot Pressure Profiles Downstream of the M3 Nozzle Throat for $Re_{o,r^*} = 330$

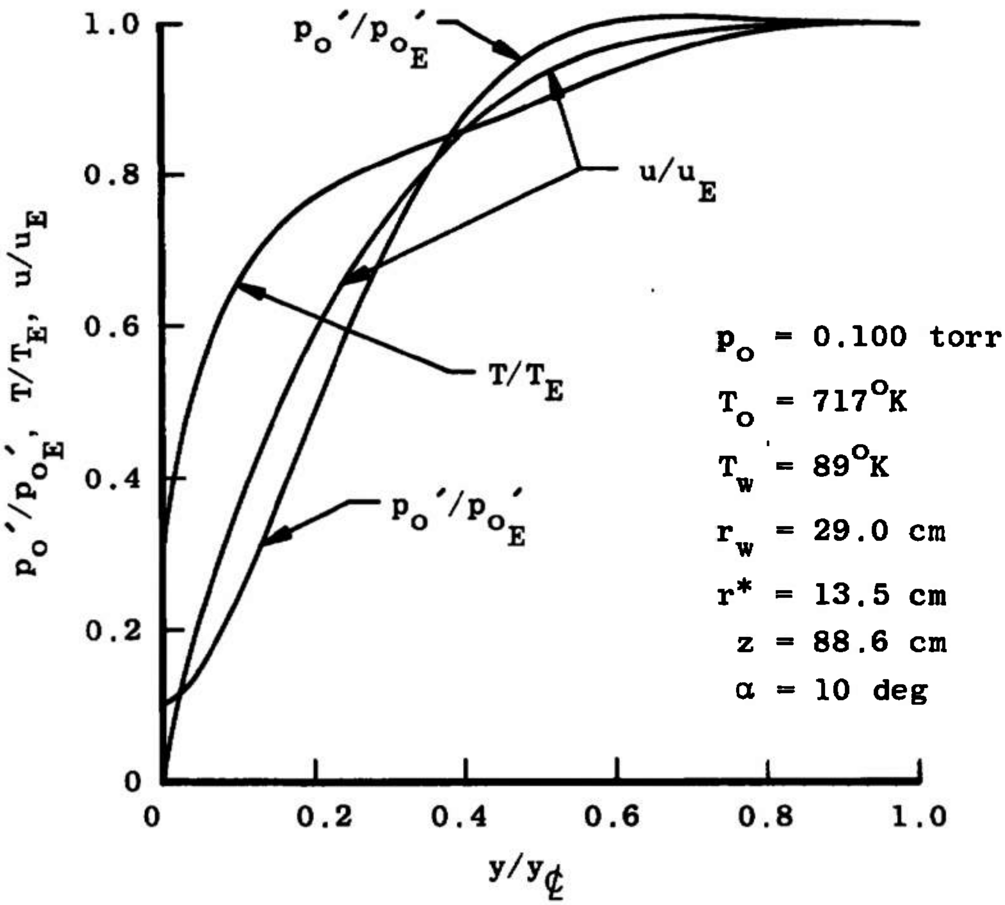

Fig. 20 Calculated Velocity, Temperature, and Pitot Pressure Profiles Downstream of the M3 Nozzle Throat for $Re_{o,r^*} = 330$

Curve	Numerical Method	Higher-Order Effects	Source
———	Beckwith and Cohen (Local Similarities, Ref. 17)	None	Ref. 16
— — — —	Incremental Flat Plate (Ref. 18)	None	Ref. 16
—— - ——	Jaffe, Lind, and Smith (Nonsimilar, Ref. 7)	None	Ref. 5
—×——×—	Patankar and Spalding (Nonsimilar, Ref. 11)	Transverse Curvature	Present

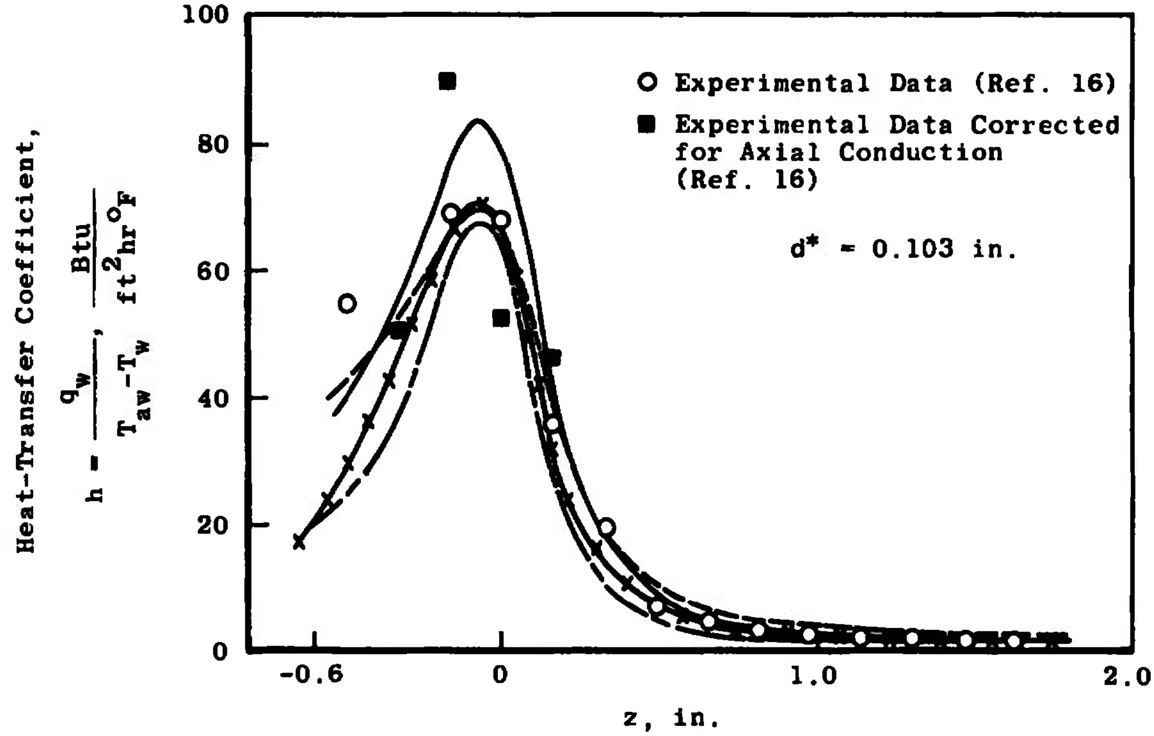

Fig. 21 Calculated and Measured Heat-Transfer Coefficients in a Low-Density Nozzle

TABLE I
CONDITIONS FOR THE NUMERICAL SOLUTIONS PRESENTED IN SECTION IV

Condition No.	γ	Pr	ζ	T_w/T_o	α, deg	A/A^*	$\bar{R}$	Re_{o,r^*}	Comment
1	9/7	3/4	3/4	1/10	10	25	3	3×10^3, 10^4, 10^5	Axisymmetric Nozzle with Transverse Curvature
2	5/3	2/3	5/7		10			5×10^3, 10^4, 2×10^4, 5×10^4, 10^5	
3	7/5	5/7	2/3		10			10^3, 3×10^3, 10^4, 3×10^4, 10^5	
4					15			3×10^3, 10^4, 10^5	
5				1/3	10			5×10^3, 10^4, 3×10^4, 10^5	
6				Adiabatic				10^4, 10^5	
7		1		1/10				3×10^3, 10^4, 3×10^4, 10^5	
8		5/7	1					10^3, 10^4, 10^5	
9		5/7	2/3					3×10^3	Axisymmetric Nozzle without Transverse Curvature
10		5/7	2/3			5	9	3×10^3	Two-Dimensional Nozzle

APPENDIX III
BOUNDARY-LAYER COMPUTER CODE

```
FORTRAN IV G LEVEL  20                    MAIN               DATE = 72286          22/52/18

              C      MAIN
  0001               COMMON /GEN/ PEI,AMI,AME,DPDX,PREF(2),PR(2),P(2),DEN,AMU,XU,XD,XP,
                    1XL,DX,INTG,CSALFA,ALPHA,XR,REORS,GAM,ZETA,PPO,TWTO,YSTART,USUP,IDI
                    2MEN,IHEAT,Z,TD,XSTEP/I/N,NP1,NP2,NP3,NEQ,NPH,KEX,KIN,KASE,KRAD/B/B
                    3ETA,GAMA(2),TAUI,TAUE,AJI(2),AJE(2),INDI(2),INDE(2)/V/U(200),F(2,2
                    400),R(200),RHO(200),OM(200),Y(200)/C/SC(200),AU(200),BU(200),CU(20
                    50),A(2,200),B(2,200),C(2,200)/D/YR(200),UR(200),RR(200),HR(200),XM
                    6(200),PITOT(200),TEMP(200)/E/DSTAR(300),XRS(300),RWRS(300),COSAL(3
                    700)
  0002               COMMON /L/ AK,ALMG
  0003        1      CONTINUE
  0004               AK=1.
  0005               INTG=0
  0006               CALL BEGIN
  0007               CALL PRE (XU,DPDX)
  0008               XTHOAT=3.14159*XR/2.
  0009               AMI=0.
  0010               AME=0.
  0011               GO TO 3
  0012        2      CALL READY
              C      THE FOLLOWING STATEMENT IS TO KILL SHOT IF PROBLEMS (LIKE MERGING)
              C      OCCUR IN SUBROUTINE READY
  0013               IF (XD.GT.XL) GO TO 13
  0014        3      CONTINUE
  0015               INTG=INTG+1
              C      CHOICE OF FORWARD STEP
  0016               DX=XSTEP*R(1)
  0017               XD=XU+DX
  0018               IF (.NOT.(XU.LT.XTHOAT.AND.XD.GT.XTHOAT)) GO TO 4
  0019               XD=XTHOAT
  0020               DX=XD-XU
  0021               ITHOAT=INTG+1
  0022        4      CONTINUE
  0023               IF (XD.LE.XL) GO TO 5
  0024               XD=XL
  0025               DX=XD-XU
  0026        5      CONTINUE
  0027               CALL PRE (XD,DPDX)
  0028               CALL ENTRN
  0029               CALL PRE (XU,DPDX)
  0030               IF (KASE.EQ.2) GO TO 6
  0031               IF (KIN.EQ.1) CALL MASS (XU,XD,AMI)
  0032               IF (KEX.EQ.1) CALL MASS (XU,XD,AME)
  0033               CALL WALL
  0034        6      CALL OUTPUT
  0035               CALL PRE (XD,DPDX)
  0036               CALL COEFF
              C      SETTING UP VELOCITIES AT A FREE BOUNDARY
              C      MODIFIED FOLLOWING STATEMENT FOR INTERNAL CORE FLOW
  0037               IF (KEX.EQ.2) U(NP3)=SQRT(2.)*SQRT(1.-PPO**((GAM-1.)/GAM))
  0038               IF (KIN.EQ.2) U(1)=SQRT(U(1)*U(1)-2.*(XD-XU)*DPDX/RHO(1))
  0039               CALL SOLVE (AU,BU,CU,U,NP3)
              C      SETTING UP VELOCITIES AT A SYMMETRY LINE
  0040               IF (KIN.NE.3) GO TO 7
  0041               U(1)=U(2)
  0042               IF (KRAD.EQ.0) U(1)=.75*U(2)+.25*U(3)
```

```
FORTRAN IV G LEVEL  20                    MAIN              DATE = 72286          22/52/18

0043       7      IF (KEX.EQ.3) U(NP3)=.75*U(NP2)+.25*U(NP1)
0044              IF (NEQ.EQ.1) GO TO 14
0045              DO 13 J=1,NPH
0046              DO 8 I=2,NP2
0047              AU(I)=A(J,I)
0048              BU(I)=B(J,I)
0049       8      CU(I)=C(J,I)
0050              DO 9 I=1,NP3
0051       9      SC(I)=F(J,I)
0052              CALL SOLVE (AU,BU,CU,SC,NP3)
0053              DO 10 I=1,NP3
0054      10      F(J,I)=SC(I)
0055              IF (KASE.EQ.2) GO TO 11
           C      SETTING UP WALL VALUES OF F
0056              IF (KIN.EQ.1.AND.INDI(J).EQ.2) F(J,1)=((1.+BETA+GAMA(J))*F(J,2)-(1
                 1.+BETA-GAMA(J))*F(J,3))*.5/GAMA(J)
0057              IF (KEX.EQ.1.AND.INDE(J).EQ.2) F(J,NP3)=((1.+BETA+GAMA(J))*F(J,NP2
                 1)-(1.+BETA-GAMA(J))*F(J,NP1))*.5/GAMA(J)
           C      SETTING UP SYMMETRY-LINE VALUES OF F
0058      11      IF (KIN.NE.3) GO TO 12
0059              F(J,1)=F(J,2)
0060              IF (KRAD.EQ.0) F(J,1)=.75*F(J,2)+.25*F(J,3)
0061      12      IF (KEX.EQ.3) F(J,NP3)=.75*F(J,NP2)+.25*F(J,NP1)
0062      13      CONTINUE
0063      14      XP=XU
0064              XRS(INTG)=XU
0065              RWPS(INTG)=R(1)
0066              COSAL(INTG)=CSALFA
0067              XU=XD
0068              PEI=PEI+DX*(R(1)*AMI-R(NP3)*AME)
           C      THE TERMINATION CONDITION
0069       1      IF (XU.LT.XL) GO TO 2
0070              CALL NEWPPO
0071              STOP
0072              END
```

```
FORTRAN IV G LEVEL  20                NEWPPO              DATE = 72286          22/52/18

0001                SUBROUTINE NEWPPO
0002                COMMON /GEN/ PEI,AMI,AME,DPDX,PREF(2),PR(2),P(2),DEN,AMU,XU,XD,XP,
                   1XL,DX,INTG,CSALFA,ALPHA,XR,REORS,GAM,ZETA,PPO,TWTO,YSTART,USUP,IDI
                   2MEN,IHEAT,Z,TO,XSTEP/E/DSTAR(300),XRS(300),RWRS(300),COSAL(300)
0003                DIMENSION FMM(300), POP(300), RIRS(300)
0004                IF (IDIMEN.EQ.0) RETURN
0005                G=GAM
0006                C1=(G+1.)/2.
0007                C2=(G-1.)/2.
0008                C3=(G+1.)/(2.*(G-1.))
0009                C4=C1**C3
0010                C5=C4*C2*C3*2.
0011                DO 1 I=1,INTG
0012         1      RIRS(I)=RWRS(I)-COSAL(I)*DSTAR(I)
0013                DO 2 I=1,INTG
0014                IF (RIRS(I).LT.RIRS(I+1)) GO TO 3
0015         2      CONTINUE
0016         3      RTHOAT=RWRS(I)-COSAL(I)*DSTAR(I)
0017                DO 14 I=1,INTG
0018                A=(RTHOAT/RIRS(I))**2
0019                IF (I-1) 4,4,6
0020         4      FM1=0.5
0021         5      B=(1.+C2*FM1**2)
0022                FM=FM1-(A*B**(C3+1.)-C4*FM1*B)/(C5*FM1**2-C4*B)
0023                IF (ABS(FM-FM1)-.00001) 13,12,12
0024         6      IF (A-1.0) 8,7,7
0025         7      FM=1.0
0026                B=(1.+C2)
0027                GO TO 13
0028         8      CONTINUE
0029                IF (FM-1.0) 9,10,10
0030         9      FM1=FM
0031                GO TO 11
0032        10      FM1=FM+0.1
0033        11      CONTINUE
0034                GO TO 5
0035        12      FM1=FM
0036                GO TO 5
0037        13      POP(I)=B**(G/(1.-G))
0038                FMM(I)=FM
0039        14      CONTINUE
0040                WRITE (6,15)
0041                WRITE (7,16) INTG
0042                WRITE (7,17) (XRS(I),POP(I),I,I=1,INTG)
0043                WRITE (6,18) (FMM(I),POP(I),DSTAR(I),XRS(I),RWRS(I),I,I=1,INTG)
0044                RETURN
             C
0045        15      FORMAT(1H1,2X,'THE DISPLACEMENT THICKNESS FROM THIS ITERATION AND
                   1THE PRESSURE DISTRIBUTION FOR THE NEXT ITERATION FOLLOWS'//,
                   28X,'M',11X,'P/PO',11X,'DS',13X,'X',12X,'RW',8X,'INTG'/)
0046        16      FORMAT(I3)
0047        17      FORMAT(1P2E12.6,53X,I3)
0048        18      FORMAT(1P5E14.5,I6)
0049                END
```

```
FORTRAN IV G LEVEL  20                 BEGIN              DATE = 72286        22/52/18

0001              SUBROUTINE BEGIN
0002              COMMON /GEN/ PEI,AMI,AME,DPOX,PREF(2),PR(2),P(2),DEN,AMU,XU,XD,XP,
                 1XL,DX,INTG,CSALFA,ALPHA,XR,REORS,GAM,ZETA,PPO,TWTO,YSTART,USUP,IDI
                 2MEN,IHEAT,Z,TO,XSTEP/I/N,NP1,NP2,NP3,NEQ,NPH,KEX,KIN,KASE,KRAD/B/B
                 3ETA,GAMA(2),TAUI,TAUE,AJI(2),AJE(2),INDI(2),INDE(2)/V/U(200),F(2,2
                 400),R(200),RHO(200),OM(200),Y(200)
            C     PROBLEM SPECIFICATION
0003              READ (5,28) KRAD,IDIMEN,NEQ,KEX,KIN,IHEAT,N
0004              READ (5,29) REORS,ZETA,PR(1),GAM,ALPHA,XR,XL,USUP,YSTART,TWTO,XSTE
                 1P
            C     IDIMEN=0 FOR PLANAR FLOW AND IDIMEN=1 FOR AXISYMMETRIC FLOW
            C     INITIAL EDGE OF BOUNDARY LAYER IS YSTART
0005              PREF(1)=PR(1)
            C     APPROXIMATE CALCULATION OF UEDGE FROM ONE DIMENSION FLOW RELATIONS
0006              UUMXX=SQRT(2./(GAM-1.))*((GAM+1.)/2.)**((GAM+1.)/(2.*(GAM-1.)))
0007              UUMXX=(1./(1.+XR))**(1+IDIMEN)/UUMXX
0008              UEDGE=UUMXX*SQRT(2.)
0009              KASE=2
0010              IF (KIN.EQ.1.OR.KEX.EQ.1) KASE=1
0011              XU=0.
0012              NPH=NEQ-1
0013              NP1=N+1
0014              NP2=N+2
0015              NP3=N+3
            C     INITIAL VELOCITY PROFILE
0016              Y(1)=0.0
0017              U(1)=0.0
0018              XNP2=NP2
0019              DELY=YSTART/XNP2
0020              DO 1 I=2,NP3
0021              Y(I)=Y(I-1)+DELY
0022              ETA=Y(I)/(DELY*XNP2)
0023              U(I)=(2.*ETA-ETA**2)*UEDGE
0024            1 CONTINUE
            C     CALCULATION OF SLIP VELOCITIES AND DISTANCES
0025              BETA=1.0
0026              GO TO (2,3,4), KIN
0027            2 U(2)=U(3)/(1.+2.*BETA)
0028              Y(2)=Y(3)*BETA/(2.+BETA)
0029              GO TO 6
0030            3 U11=U(1)*U(1)
0031              U13=U(1)*U(3)
0032              U33=U(3)*U(3)
0033              SQ=84.*U11-12.*U13+9.*U33
0034              U(2)=(16.*U11-4.*U13+U33)/(2.*(U(1)+U(3))+SQRT(SQ))
0035              Y(2)=Y(3)*(U(2)+U(3)-2.*U(1))*.5/(U(2)+U(3)+U(1))
0036              GO TO 6
0037            4 IF (KRAD.NE.0) GO TO 5
0038              U(2)=(4.*U(1)-U(3))/3.
0039              Y(2)=0.
0040              GO TO 6
0041            5 U(2)=U(1)
0042              Y(2)=Y(3)/3.
0043            6 GO TO (7,8,9), KEX
0044            7 U(NP2)=U(NP1)/(1.+2.*BETA)
0045              Y(NP2)=Y(NP3)-(Y(NP3)-Y(NP1))*BETA/(2.+BETA)
```

```
FORTRAN IV G LEVEL  20                BEGIN              DATE = 72286          22/52/18

0046                GO TO 10
0047        8       U11=U(NP1)*U(NP1)
0048                U13=U(NP1)*U(NP3)
0049                U33=U(NP3)*U(NP3)
0050                SQ=84.*U33-12.*U13+9.*U11
0051                U(NP2)=(16.*U33-4.*U13+U11)/(2.*(U(NP1)+U(NP3))+SQRT(SQ))
0052                Y(NP2)=Y(NP3)-(Y(NP3)-Y(NP1))*(U(NP2)+U(NP1)-2.*U(NP3))*.5/(U(NP2)
                   1+U(NP1)+U(NP3))
0053                GO TO 10
0054        9       U(NP2)=(4.*U(NP3)-U(NP1))/3.
0055                Y(NP2)=Y(NP3)
0056       10       CONTINUE
0057                IF (NEQ.EQ.1) GO TO 20
0058                DO 19 J=1,NPH
            C       INITIAL PROFILES OF OTHER DEPENDENT VARIABLES
0059                DO 11 I=1,NP3
0060                ETA=Y(I)/(DELY*XNP2)
0061                F(J,I)=TWTO+(2.*ETA-ETA**2)*(1.-TWTO)
0062       11       CONTINUE
            C       CALCULATION OF CORRESPONDING SLIP VALUES
0063                GAMA(J)=1.0
0064                GO TO (12,13,14), KIN
0065       12       F(J,2)=F(J,1)+(F(J,3)-F(J,1))*(1.+BETA-GAMA(J))/(1.+BETA+GAMA(J))
0066                GO TO 15
0067       13       G=(U(2)+U(3)-8.*U(1))/(5.*(U(2)+U(3))+8.*U(1))
0068                GF=(1.-PREF(J))/(1.+PREF(J))
0069                GF=(G+GF)/(1.+G*GF)
0070                F(J,2)=F(J,3)*GF+(1.-GF)*F(J,1)
0071                GO TO 15
0072       14       F(J,2)=F(J,1)
0073                IF (KRAD.EQ.0) F(J,2)=(4.*F(J,1)-F(J,3))/3.
0074       15       GO TO (16,17,18), KEX
0075       16       F(J,NP2)=F(J,NP3)+(F(J,NP1)-F(J,NP3))*(1.+BETA-GAMA(J))/(1.+BETA+G
                   1AMA(J))
0076                GO TO 19
0077       17       G=(U(NP2)+U(NP1)-8.*U(NP3))/(5.*(U(NP2)+U(NP1))+8.*U(NP3))
0078                GF=(1.-PREF(J))/(1.+PREF(J))
0079                GF=(G+GF)/(1.+G*GF)
0080                F(J,NP2)=F(J,NP1)*GF+(1.-GF)*F(J,NP3)
0081                GO TO 19
0082       18       F(J,NP2)=(4.*F(J,NP3)-F(J,NP1))/3.
0083       19       CONTINUE
0084       20       CONTINUE
0085                CALL DENSTY
            C       CALCULATION OF RADII
0086                CALL RAD (XU,R(1),CSALFA)
0087                IF (CSALFA.EQ.0..OR.KRAD.EQ.0) GO TO 22
0088                DO 21 I=2,NP3
0089       21       R(I)=R(1)-Y(I)*CSALFA
            C       CHANGE MADE IN STATEMENT NUMBER 28 FOR INTERNAL FLOW
0090                GO TO 24
0091       22       DO 23 I=2,NP3
0092       23       R(I)=R(1)
0093       24       CONTINUE
            C       CALCULATION OF OMEGA VALUES
0094                OM(1)=0.
```

```
FORTRAN IV G LEVEL  20                    BEGIN              DATE = 72286           22/52/18

0095                   OM(2)=0.
0096                   DO 25 I=3,NP2
0097          25       OM(I)=OM(I-1)+.5*(RHO(I)*U(I)*R(I)+RHO(I-1)*U(I-1)*R(I-1))*(Y(I)-Y
                      1(I-1))
0098                   PEI=OM(NP2)
0099                   DO 26 I=3,NP1
0100          26       OM(I)=OM(I)/PEI
0101                   OM(NP2)=1.
0102                   OM(NP3)=1.
0103                   IF (NEQ.EQ.1) RETURN
0104                   DO 27 J=1,NPH
0105                   IF (KEX.EQ.1) INDE(J)=1
0106                   IF (KIN.EQ.1) INDI(J)=1
0107          27       CONTINUE
0108                   RETURN
               C
0109          28       FORMAT(6I1,I3)
0110          29       FORMAT (8E10.0)
0111                   END
```

```
FORTRAN IV G LEVEL  20                 COEFF              DATE = 72286          22/52/18

0001                 SUBROUTINE COEFF
0002                 COMMON /GEN/ PEI,AMI,AME,DPDX,PREF(2),PR(2),P(2),DEN,AMU,XU,XD,XP,
                    1XL,OX,INTG,CSALFA,ALPHA,XP,REURS,GAM,ZETA,PPO,TWTO,YSTART,USUP,IDI
                    2MEN,IHEAT,Z,TO,XSTEP/I/N,NP1,NP2,NP3,NEQ,NPH,KEX,KIN,KASE,KRAD/B/B
                    3ETA,GAMA(2),TAUI,TAUE,AJI(2),AJE(2),INDI(2),INDE(2)/V/U(200),F(2,2
                    400),R(200),RHO(200),OM(200),Y(200)/C/SC(200),AU(200),BU(200),CU(20
                    50),A(2,200),B(2,200),C(2,200)
0003                 COMMON /L/ AK,ALMG
0004                 DIMENSION G1(200), G2(200), G3(200), D(2,200), S1(200), S2(200), S
                    13(200)
            C        CALCULATION OF SMALL C 'S
0005                 DO 1 I=2,NP1
0006                 RA=.5*(R(I+1)+R(I))
0007                 RH=.5*(RHO(I+1)+RHO(I))
0008                 UM=.5*(U(I+1)+U(I))
0009                 CALL VEFF (I,I+1,EMU)
0010        1        SC(I)=RA*RA*RH*UM*EMU/(PEI*PEI)
            C        THE CONVECTION TERM
0011                 SA=R(1)*AMI/PEI
0012                 SB=(R(NP3)*AME-R(1)*AMI)/PEI
0013                 DX=XD-XU
0014                 DO 4 I=3,NP1
0015                 OMD=OM(I+1)-OM(I-1)
0016                 P2=.25/DX
0017                 P3=P2/OMD
0018                 P1=(OM(I+1)-OM(I))*P3
0019                 P3=(OM(I)-OM(I-1))*P3
0020                 P2=3.*P2
0021                 Q=SA/OMD
0022                 R2=-SB*.25
0023                 R3=P2/OMD
0024                 R1=-(OM(I+1)+3.*OM(I))*R3
0025                 R3=(OM(I-1)+3.*OM(I))*R3
0026                 G1(I)=P1+Q+R1
0027                 G2(I)=P2+R2
0028                 G3(I)=P3-Q+R3
0029                 CU(I)=-P1*U(I+1)-P2*U(I)-P3*U(I-1)
            C        THE DIFFUSION TERM
0030                 AU(I)=2./OMD
0031                 BU(I)=SC(I-1)*AU(I)/(OM(I)-OM(I-1))
0032                 AU(I)=SC(I)*AU(I)/(OM(I+1)-OM(I))
0033                 IF (NEQ.EQ.1) GO TO 3
0034                 DO 2 J=1,NPH
0035                 C(J,I)=-P1*F(J,I+1)-P2*F(J,I)-P3*F(J,I-1)
0036                 CALL SOURCE (J,I,CS,D(J,I))
0037                 C(J,I)=-C(J,I)+CS-F(J,I)*D(J,I)
0038                 A(J,I)=AU(I)/PREF(J)
0039                 B(J,I)=BU(I)/PREF(J)
0040        2        CONTINUE
            C        SOURCE TERM FOR VELOCITY EQUATION
0041        3        S1(I)=DPDX*DX
0042                 S2(I)=P2*S1(I)/(RHO(I)*U(I))
0043                 S3(I)=P3*S1(I)/(RHO(I-1)*U(I-1))
0044                 S1(I)=P1*S1(I)/(RHO(I+1)*U(I+1))
0045                 CU(I)=-CU(I)-2.*(S1(I)+S2(I)+S3(I))
0046                 S1(I)=S1(I)/U(I+1)
```

```
FORTRAN IV G LEVEL  20                COEFF              DATE = 72286          22/52/18

 0047                 S2(I)=S2(I)/U(I)                                              D  57
 0048                 S3(I)=S3(I)/U(I-1)                                            D  58
 0049         4       CONTINUE                                                      D  59
              C       COEFFICIENTS IN THE FINAL FORM                                D  60
 0050                 DO 5 I=3,NP1                                                  D  61
 0051                 RL=1./(G2(I)+AU(I)+BU(I)-S2(I))                               D  62
 0052                 AU(I)=(AU(I)+S1(I)-G1(I))*RL                                  D  63
 0053                 BU(I)=(BU(I)+S3(I)-G3(I))*RL                                  D  64
 0054         5       CU(I)=CU(I)*RL                                                D  65
 0055                 IF (NEU.EQ.1) GO TO 7                                         D  66
 0056                 DO 6 J=1,NPH                                                  D  67
 0057                 DO 6 I=3,NP1                                                  D  68
 0058                 RL=1./(G2(I)+A(J,I)+B(J,I)-D(J,I))                            D  69
 0059                 A(J,I)=(A(J,I)-G1(I))*RL                                      D  70
 0060                 B(J,I)=(B(J,I)-G3(I))*RL                                      D  71
 0061         6       C(J,I)=C(J,I)*RL                                              D  72
 0062         7       CALL SLIP                                                     D  73
 0063                 RETURN                                                        D  74
 0064                 END                                                           D  75-
```

```
FORTRAN IV G LEVEL  20                  READY                  DATE = 72286            22/52/18

0001                   SUBROUTINE READY
0002                   COMMON /GEN/ PEI,AMI,AME,OPDX,PREF(2),PR(2),P(2),DEN,AMU,XU,XD,XP,
                      1XL,DX,INTG,CSALFA,ALPHA,XR,REORS,GAM,ZETA,PPO,THTO,YSTART,USUP,IDI
                      2MEN,IHEAT,Z,TO,XSTEP/V/U(200),F(2,200),R(200),RHO(200),OM(200),Y(2
                      300)/I/N,NP1,NP2,NP3,NEQ,NPH,KEX,KIN,KASE,KRAD/B/BETA,GAMA(2),TAUI,
                      4TAUE,AJI(2),AJE(2),INDI(2),INDE(2)
0003                   CALL DENSTY
0004                   CALL RAD (XU,R(1),CSALFA)
                C      Y NEAR THE I BOUNDARY
0005                   GO TO (1,2,3), KIN
0006            1      Y(2)=(1.+BETA)*OM(3)*4./((3.*RHO(2)+RHO(3))*(U(2)+U(3)))
0007                   GO TO 4
0008            2      Y(2)=12.*OM(3)/((3.*RHO(2)+RHO(3))*(U(2)+U(3)+4.*U(1)))
0009                   GO TO 4
0010            3      Y(2)=.5*OM(3)/(RHO(1)*U(1))
0011            4      Y(3)=Y(2)+.25*OM(3)*(1./(RHO(3)*U(3))+2./(RHO(3)*U(3)+RHO(2)*U(2))
                      1)
                C      Y 'S FOR INTERMEDIATE GRID POINTS
0012                   DO 5 I=4,NP1
0013            5      Y(I)=Y(I-1)+.5*(OM(I)-OM(I-1))*(1./(RHO(I)*U(I))+1./(RHO(I-1)*U(I-
                      11)))
                C      Y NEAR THE E BOUNDARY
0014                   Y(NP2)=Y(NP1)+.25*(OM(NP2)-OM(NP1))*(1./(RHO(NP1)*U(NP1))+2./(RHO(
                      1NP1)*U(NP1)+RHO(NP2)*U(NP2)))
0015                   GO TO (6,7,8), KEX
0016            6      Y(NP3)=Y(NP2)+(1.+BETA)*(OM(NP2)-OM(NP1))*4./((RHO(NP1)+3.*RHO(NP2
                      1))*(U(NP1)+U(NP2)))
0017                   GO TO 9
0018            7      Y(NP3)=Y(NP2)+12.*(OM(NP2)-OM(NP1))/((RHO(NP1)+3.*RHO(NP2))*(U(NP2
                      1)+U(NP1)+4.*U(NP3)))
0019                   GO TO 9
0020            8      Y(NP3)=Y(NP2)+.5*(OM(NP2)-OM(NP1))/(RHO(NP3)*U(NP3))
0021            9      IF (CSALFA.EQ.0..OR.KRAD.EQ.0) GO TO 11
                C      XXX IS USED TO KILL SHOT IF NECESSARY
0022                   DO 10 I=2,NP3
0023                   XXX=R(1)*R(1)-2.*Y(I)*PEI*CSALFA
0024                   IF (XXX.LT.0.0) XD=2.*XL
0025                   IF (XXX.LT.0.0) GO TO 14
0026           10      Y(I)=2.*Y(I)*PEI/(R(1)+SQRT(R(1)*R(1)-2.*Y(I)*PEI*CSALFA))
                C      CHANGED SIGN OF 2 IN THE DENOMINATOR OF ABOVE FOR INTERNAL FLOW
0027                   GO TO 13
0028           11      DO 12 I=2,NP3
0029           12      Y(I)=PEI*Y(I)/R(1)
0030           13      Y(2)=2.*Y(2)-Y(3)
0031                   Y(NP2)=2.*Y(NP2)-Y(NP1)
                C      CALCULATION OF RADII
0032                   DO 14 I=2,NP3
0033                   IF (KRAD.EQ.0) R(I)=R(1)
0034                   IF (KRAD.NE.0) R(I)=R(1)-Y(I)*CSALFA
                C      CHANGED SIGN IN EXPRESSION ABOVE FOR INTERNAL FLOW
0035           14      CONTINUE
0036                   IF (R(NP3).LE.0.0) XD=2.*XL
0037                   IF (Y(NP3).LT.0.0) XD=2.*XL
0038                   RETURN
0039                   END
```

```
FORTRAN IV G LEVEL  20                 DENSTY              DATE = 72286         22/52/18

0001                SUBROUTINE DENSTY
0002                COMMON /GEN/ PEI,AMI,AME,DPDX,PREF(2),PR(2),P(2),DEN,AMU,XU,XD,XP,
                   1XL,DX,INTG,CSALFA,ALPHA,XR,REORS,GAM,ZETA,PPO,TWTO,YSTART,USUP,IDI
                   2MFN,IHEAT,Z,TO,XSTEP/V/U(200),F(2,200),R(200),RHO(200),OM(200),Y(2
                   300)/I/N,NP1,NP2,NP3,NEQ,NPH,KEX,KIN,KASE,KRAD
0003                TNP3=F(1,NP3)-U(NP3)**2/2.
0004                RHONP3=TNP3**(1./(GAM-1.))
0005                DO 1 I=1,NP3
0006                T=F(1,I)-U(I)**2/2.
0007           1    RHO(I)=RHONP3*TNP3/T
0008                RETURN
0009                END
```

```
FORTRAN IV G LEVEL  20                 ENTRN               DATE = 72286         22/52/18

0001                SUBROUTINE ENTRN
0002                COMMON /GEN/ PEI,AMI,AME,DPDX,PREF(2),PR(2),P(2),DEN,AMU,XU,XD,XP,
                   1XL,DX,INTG,CSALFA,ALPHA,XR,REORS,GAM,ZETA,PPO,TWTO,YSTART,USUP,IDI
                   2MFN,IHEAT,Z,TO,XSTEP/V/U(200),F(2,200),R(200),RHO(200),OM(200),Y(2
                   300)/I/N,NP1,NP2,NP3,NEQ,NPH,KEX,KIN,KASE,KRAD
0003           1    GO TO (2,3,6), KEX
0004           2    RETURN
0005           3    CONTINUE
               C    THE FOLLOWING AME IS FOR LAMINAR FLOW
0006                IF (INTG.NE.1) GO TO 5
0007                DO 4 I=1,NP3
0008                IF (OM(I).GT.0.9) N9=I
0009                IF (OM(I).GT.0.9) I=NP3
0010           4    CONTINUE
0011                DOM=OM(N9)-OM(N9-1)
0012                DOM9=OM(N9)-0.9
0013           5    CONTINUE
0014                U9=U(N9)-DOM9/DOM*(U(N9)-U(N9-1))
0015                TERMB=(U(N9)-U(N9-1))/DOM
0016                R9=R(N9)-DOM9/DOM*(R(N9)-R(N9-1))
0017                RHO9=RHO(N9)-DOM9/DOM*(RHO(N9)-RHO(N9-1))
0018                VIS9=VISCO(N9)-DOM9/DOM*(VISCO(N9)-VISCO(N9-1))
0019                CUUP=R(N9)*R(N9)*RHO(N9)*U(N9)*VISCO(N9)
0020                CUUP=CUUP+R9*R9*RHO9*U9*VIS9
0021                CUUP=CUUP/(2.*PEI)
0022                CUUM=R(N9-1)*R(N9-1)*RHO(N9-1)*U(N9-1)*VISCO(N9-1)
0023                CUUM=CUUM+R9*R9*RHO9*U9*VIS9
0024                CUUM=CUUM/(2.*PEI)
0025                G5=2.*CUUP/(DOM*DOM9)
0026                G6=2.*CUUM/(DOM*(0.9-OM(N9-1)))
0027                TERMA=G5*(U(N9)-U9)-G6*(U9-U(N9-1))
0028                TERMA=TERMA/TERMB
0029                U9WIG=USUP*SQRT(2.)*SQRT(1.-PPO**((GAM-1.)/GAM))
               C    USUP IS READ-IN IN BEGIN     IT SUPPRESSES THE B.L.
0030                TERMC=(U9WIG-U9)/DX+DPDX/(RHO9*U9)
0031                TERMC=TERMC*PEI/TERMB
0032                AME=TERMA-TERMC
0033                AME=AME-0.1*R(1)*AMI
0034                AME=AME/(0.9*R(NP3))
0035                RETURN
0036           6    AME=0.
0037                RETURN
0038                END
```

```
FORTRAN IV G LEVEL  20                  FBC                  DATE = 72286            22/52/18

 0001                 SUBROUTINE FBC (X,J,IND,AJFS)
 0002                 COMMON /GEN/ PEI,AMI,AME,DPDX,PREF(2),PR(2),P(2),DEN,AMU,XU,XD,XP,
                     1XL,DX,INTG,CSALFA,ALPHA,XR,REORS,GAM,ZETA,PPO,TWTO,YSTART,USUP,IDI
                     2MEN,IHEAT,Z,TO,XSTEP
              C       TW IS PRESCRIBED IF IHEAT = 1 -- QDOT IS PRESCRIBED IF NOT 1
 0003                 IND=1
 0004                 AJFS=TWTO
 0005                 IF (IHEAT.EQ.1) GO TO 1
 0006                 IND=2
 0007                 AJFS=0.0
 0008         1       CONTINUE
 0009                 RETURN
 0010                 END
```

```
FORTRAN IV G LEVEL  20                  MASS                 DATE = 72286            22/52/18

 0001                 SUBROUTINE MASS (XU,XD,AM)
              C       APPLICABLE TO AN IMPERMEABLE-WALL SITUATION
 0002                 AM=0.
 0003                 RETURN
 0004                 END
```

```
FORTRAN IV G LEVEL  20                    OUTPUT              DATE = 72286          22/52/18

0001                 SUBROUTINE OUTPUT
0002                 COMMON /GEN/ PEI,AMI,AME,DPDX,PREF(2),PR(2),P(2),DEN,AMU,XU,XD,XP,
                    1XL,DX,INTG,CSALFA,ALPHA,XR,REORS,GAM,ZETA,PPU,TWTO,YSTART,USUP,IDI
                    2MEN,IHEAT,Z,TU,XSTEP/V/U(200),F(2,200),R(200),RHO(200),OM(200),Y(2
                    300)/C/SC(200),AU(200),BU(200),CU(200),A(2,200),B(2,200),C(2,200)/D
                    4/YP(200),UR(200),RR(200),HR(200),XM(200),PITOT(200),TEMP(200)/E/DS
                    5TAR(300),XRS(300),RWRS(300),COSAL(300)/I/N,NP1,NP2,NP3,NEQ,NPH,KEX
                    6,KIN,KASE,KRAD/B/BETA,GAMA(2),TAUI,TAUE,AJI(2),AJE(2),INDI(2),INDE
                    7(2)
0003                 IF (INTG.NE.1) GO TO 1
0004                 AL=ALPHA*180./3.14159265
0005                 WRITE (6,7) (OM(I),I=1,NP3)
0006                 WRITE (6,6) KRAD,IDIMEN,NEQ,KEX,KIN,IHEAT,N
0007          1      CONTINUE
0008                 DPDXG=DPDX*GAM/(GAM-1.)
0009                 IF (KRAD.EQ.0) DSTAR(INTG)=Y(NP3)-PEI/(R(1)*RHO(NP3)*U(NP3))
0010                 IF (KRAD.EQ.0) GO TO 2
0011                 DSTAR(INTG)=R(1)-SQRT(R(1)**2-2.*CSALFA*(R(1)*Y(NP3)-0.5*CSALFA*Y(
                    1NP3)**2-PEI/(RHO(NP3)*U(NP3))))
0012                 IF (CSALFA.NE.0.0) DSTAR(INTG)=DSTAR(INTG)/CSALFA
0013          2      CONTINUE
0014                 IF (FLOAT(INTG-1)/5..NE.FLOAT((INTG-1)/5)) RETURN
0015                 DO 3 I=1,NP3
0016                 TEMP(I)=F(1,I)-U(I)**2/2.
0017                 XM(I)=U(I)/SQRT((GAM-1.)*TEMP(I))
0018                 XSQ=XM(I)**2
0019                 IF (XM(I).LE.1.0) PITOT(I)=(1.+(GAM-1.)*XSQ/2.)**(GAM/(GAM-1.))
0020                 IF (XM(I).LE.1.0) GO TO 3
0021                 PITOT(I)=((GAM+1.)*XSQ/2.)**(GAM/(GAM-1.))
0022                 PITOT(I)=PITOT(I)*((GAM+1.)/(2.*GAM*XSQ-GAM+1.))**(1./(GAM-1.))
0023          3      CONTINUE
0024                 SQ2=SQRT(2.)
0025                 DO 4 I=1,NP3
0026                 PITOT(I)=PITOT(I)/PITOT(NP3)
0027                 YR(I)=Y(I)*CSALFA/R(1)
0028                 UR(I)=U(I)/U(NP3)
0029                 RR(I)=RHO(I)/RHO(NP3)
0030                 HR(I)=U(I)/SQ2
0031          4      CONTINUE
0032                 WRITE (6,8)
0033                 WRITE (6,12) INTG,XU,Z,REORS,GAM,PR(1),ZETA,TWTO,AL,XR,XL
0034                 WRITE (6,13) NP3,DSTAR(INTG),PEI,AME,DPDXG,DX,CSALFA,USUP,PPO,TAUI
                    1,AJI(1)
0035                 WRITE (6,9)
0036                 DO 5 I=1,NP3,2
0037                 WRITE (6,11) (Y(I),F(1,I),UR(I),HR(I),R(I),RHO(I),YR(I),XM(I),TEMP
                    1(I),RR(I),PITOT(I))
0038          5      CONTINUE
0039                 WRITE (6,10) (Y(NP3),F(1,NP3),UR(NP3),HR(NP3),R(NP3),RHO(NP3),YR(N
                    1P3),XM(NP3),TEMP(NP3),RR(NP3),PITOT(NP3))
0040                 WRITE (6,9)
0041                 RETURN
              C
0042          6      FORMAT(////////,20X,'THE INPUT FLAGS ARE',///,25X,'KRAD    = ',I1,
                    1//,25X,'IDIMEN = ',I1,//,25X,'NEQ      = ',I1,//,25X,'KEX      = ',I1,
                    2//,25X,'KIN      = ',I1,//,25X,'IHEAT   = ',I1,//,25X,'N        = ',I3)
```

```
FORTRAN IV G LEVEL  20                OUTPUT              DATE = 72286         22/52/18

  0043          7       FORMAT(24H1THE VALUES OF OMEGA ARE/(1P10E11.4))
  0044          8       FORMAT(1H1,4X,'INTG',9X,'XU',11X,'Z',9X,'REORS',7X,'GAMMA',8X,'PR'
                       1,9X,'ZETA',8X,'TW/TO',7X,'ALPHA',8X,'XR',10X,'XL'/,5X,'NP3',9X,'DS
                       2TAR',8X,'PEI',9X,'AME',8X,'DP/DX',8X,'DX',8X,'COSALF',7X,'USUP',8X
                       3,'P/PO',8X,'TAUI',7X,'AJI(1)'/)
  0045          9       FORMAT(6X,'Y',9X,'H/HO',9X,'U/UE',8X,'U/UM',9X,'R',10X,'RHO',10X,
                       1'Y/R',9X,'M',11X,'T',10X,'N/NE',7X,'PITOT'/)
  0046         10       FORMAT(1P11E12.5,/)
  0047         11       FORMAT(1P11E12.5)
  0048         12       FORMAT(I8,4X,1P10E12.4)
  0049         13       FORMAT(I8,4X,1P10E12.4,//)
  0050                  END
```

```
FORTRAN IV G LEVEL  20                PRE                 DATE = 72286         22/52/18

  0001                  SUBROUTINE PRE (X,DPDXX)
  0002                  COMMON /GEN/ PEI,AMI,AME,DPDX,PREF(2),PR(2),P(2),DEN,AMU,XU,XD,XP,
                       1XL,DX,INTG,CSALFA,ALPHA,XR,REORS,GAM,ZETA,PPO,TWTO,YSTART,USUP,IDI
                       2MEN,IHEAT,Z,TO,XSTEP/V/U(200),F(2,200),R(200),RHO(200),OM(200),Y(2
                       300)/I/N,NP1,NP2,NP3,NEQ,NPH,KEX,KIN,KASE,KRAD
  0003                  DIMENSION XX(300), POP(300)
  0004                  IF (INTG.NE.0) GO TO 1
  0005                  READ (5,3) LMAX
  0006                  READ (5,4) (XX(L),POP(L),L=1,LMAX)
  0007                  WRITE (6,5)
  0008                  WRITE (6,6) (XX(L),POP(L),L,L=1,LMAX)
  0009          1       CONTINUE
  0010                  L=1
  0011          2       CONTINUE
  0012                  L=L+1
  0013                  IF (XX(L).LT.X) GO TO 2
  0014                  DPDX=(POP(L)-POP(L-1))/(XX(L)-XX(L-1))
  0015                  PPO=POP(L-1)+DPDX*(X-XX(L-1))
  0016                  DPDXX=DPDX
  0017                  DPDXX=DPDX*(GAM-1.)/GAM
  0018                  RETURN
                C
  0019          3       FORMAT(I3)
  0020          4       FORMAT(2E12.0)
  0021          5       FORMAT(1H1,/,8X,'X',12X,'P/PO',/)
  0022          6       FORMAT(1P2E14.5,I6)
  0023                  END
```

```
FORTRAN IV G LEVEL  20                    RAD                   DATE = 72286            22/52/18

 0001                 SUBROUTINE RAD (X,R1,CALPHA)
 0002                 COMMON /GEN/ PEI,AMI,AME,DPDX,PREF(2),PR(2),P(2),DEN,AMU,XU,XD,XP,
                     1XL,DX,INTG,CSALFA,ALPHA,XR,REORS,GAM,ZETA,PPU,TWTO,YSTART,USUP,IDI
                     2MEN,IHEAT,Z,TO,XSTEP/V/U(200),F(2,200),R(200),RHO(200),OM(200),Y(2
                     3OO)/I/N,NP1,NP2,NP3,NEQ,NPH,KEX,KIN,KASE,KRAD
            C         APPLICABLE TO NOZZLES WITH CONSTANT LONGITUDINAL RADIUS OF
            C         CURVATURE OF THE CONVERGING SECTION- CONSTANT WALL HALF ANGLE OF
            C         DIVERGING SECTION-AND WALL SLOPES MATCHED DOWNSTREAM OF THE THROAT
 0003                 IF (INTG.NE.0) GO TO 1
 0004                 PI2=3.14159265/2.
 0005                 ALPHA=ALPHA*PI2/90.
 0006                 COSALF=COS(ALPHA)
 0007                 SINALF=SIN(ALPHA)
 0008                 ZWIG=XR*(1.+SINALF)
 0009                 XWIG=XR*(PI2+ALPHA)
 0010                 RWIG=1.+XR*(1.-COSALF)
 0011       1         CONTINUE
 0012                 IF (X.GE.XWIG) GO TO 2
 0013                 R(1)=1.+XR*(1.-SIN(X/XR))
 0014                 CSALFA=SIN(X/XR)
 0015                 CALPHA=CSALFA
 0016                 R1=R(1)
 0017                 ZZ=XR*(1.-COS(X/XR))
 0018                 GO TO 3
 0019       2         CONTINUE
 0020                 R(1)=(X-XWIG)*SINALF+RWIG
 0021                 CSALFA=COSALF
 0022                 CALPHA=CSALFA
 0023                 R1=R(1)
 0024                 ZZ=(X-XWIG)*CSALFA+ZWIG
 0025       3         CONTINUE
 0026                 IF((DIMEN.EQ.0)R1=1.
 0027                 ZZ=ZZ-XR
 0028                 Z=ZZ
 0029                 RETURN
 0030                 END
```

```
FORTRAN IV G LEVEL  20                  SLIP                   DATE = 72286          22/52/18

0001            SUBROUTINE SLIP
0002            COMMON /GEN/ PEI,AMI,AME,DPDX,PREF(2),PR(2),P(2),DEN,AMU,XU,XD,XP,
               1XL,DX,INTG,CSALFA,ALPHA,XR,REDRS,GAM,ZETA,PPO,TWTO,YSTART,USUP,IDI
               2MEN,IHEAT,Z,TO,XSTEP/I/N,NP1,NP2,NP3,NEQ,NPH,KEX,KIN,KASE,KRAD/V/U
               3(200),F(2,200),R(200),RHO(200),OM(200),Y(200)/B/BETA,GAMA(2),TAUI,
               4TAUE,AJI(2),AJE(2),INDI(2),INDE(2)
0003            COMMON /L/ AK,ALMG/C/SC(200),AU(200),BU(200),CU(200),A(2,200),B(2,
               1200),C(2,200)
          C     SLIP COEFFICIENTS NEAR THE I BOUNDARY FOR VELOCITY EQUATION
0004            CU(2)=0.
0005            CU(NP2)=0.
0006            GO TO (1,2,3), KIN
0007      1     BU(2)=0.
0008            AU(2)=1./(1.+2.*BETA)
0009            GO TO 5
0010      2     SQ=84.*U(1)*U(1)-12.*U(1)*U(3)+9.*U(3)*U(3)
0011            BU(2)=8.*(2.*U(1)+U(3))/(2.*U(1)+7.*U(3)+SQRT(SQ))
0012            AU(2)=1.-BU(2)
0013            GO TO 5
0014      3     BU(2)=0.
0015            CALL VEFF (2,3,EMU)
0016            AK1=1./DX-DPDX/(RHO(1)*U(1)*U(1))
0017            AK2=-U(1)*AK1+DPDX/(RHO(1)*U(1))
0018            AJ=RHO(1)*U(1)*.25*(Y(2)+Y(3))**2/EMU
0019            IF (KRAD.EQ.0) GO TO 4
0020            AU(2)=2./(2.+AJ*AK1)
0021            CU(2)=-.5*AJ*AK2*AU(2)
0022            GO TO 5
0023      4     CU(2)=1./(2.+3.*AJ*AK1)
0024            AU(2)=CU(2)*(2.-AJ*AK1)
0025            CU(2)=-CU(2)*4.*AJ*AK2
          C     SLIP COEFFICIENTS NEAR THE E BOUNDARY FOR VELOCITY EQUATION
0026      5     GO TO (6,7,8), KEX
0027      6     AU(NP2)=0.
0028            BU(NP2)=1./(1.+2.*BETA)
0029            GO TO 9
0030      7     SQ=84.*U(NP3)*U(NP3)-12.*U(NP3)*U(NP1)+9.*U(NP1)*U(NP1)
0031            AU(NP2)=8.*(2.*U(NP3)+U(NP1))/(2.*U(NP3)+7.*U(NP1)+SQRT(SQ))
0032            BU(NP2)=1.-AU(NP2)
0033            GO TO 9
0034      8     AU(NP2)=0.
0035            CALL VEFF (NP1,NP2,EMU)
0036            BK1=1./DX-DPDX/(RHO(NP3)*U(NP3)*U(NP3))
0037            BK2=-U(NP3)*BK1+DPDX/(RHO(NP3)*U(NP3))
0038            BJ=RHO(NP3)*U(NP3)*.25*(2.*Y(NP3)-Y(NP1)-Y(NP2))**2/EMU
0039            CU(NP2)=1./(2.+3.*BJ*BK1)
0040            BU(NP2)=CU(NP2)*(2.-BJ*BK1)
0041            CU(NP2)=-CU(NP2)*4.*BJ*BK2
0042      9     IF (NEQ.EQ.1) RETURN
          C     SLIP COEFFICIENTS NEAR THE I BOUNDARY FOR OTHER EQUATIONS
0043            DO 20 J=1,NPH
0044            C(J,2)=0.
0045            C(J,NP2)=0.
0046            GO TO (10,12,13), KIN
0047     10     CALL FBC (XD,J,INDI(J),QI)
0048            IF (INDI(J).EQ.1) GO TO 11
```

```
FORTRAN IV G LEVEL  20                SLIP              DATE = 72286          22/52/18

 0049                AJI(J)=QI
 0050                A(J,2)=1.
 0051                B(J,2)=0.
 0052                C(J,2)=8.*(1.+2.*BETA)*PREF(J)*AJI(J)/(AK*AK*BETA*(1.+BETA)*(1.+BE
                    1TA)*(3.*RHO(2)+RHO(3))*U(3))
 0053                GO TO 15
 0054         11     F(J,1)=QI
 0055                A(J,2)=(1.+BETA-GAMA(J))/(1.+BETA+GAMA(J))
 0056                B(J,2)=1.-A(J,2)
 0057                GO TO 15
 0058         12     A(J,2)=(U(2)+U(3)-8.*U(1))/(5.*(U(2)+U(3))+8.*U(1))
 0059                GF=(1.-PREF(J))/(1.+PREF(J))
 0060                A(J,2)=(A(J,2)+GF)/(1.+A(J,2)*GF)
 0061                B(J,2)=1.-A(J,2)
 0062                GO TO 15
 0063         13     B(J,2)=0.
 0064                CALL SOURCE (J,1,CS,DS)
 0065                AK1=1./DX-DS
 0066                AK2=-AK1*F(J,1)-CS
 0067                AJF=AJ*PREF(J)
 0068                IF (KRAD.EQ.0) GO TO 14
 0069                A(J,2)=2./(2.+AJF*AK1)
 0070                C(J,2)=-.5*AJF*AK2*A(J,2)
 0071                GO TO 15
 0072         14     C(J,2)=1./(2.+3.*AJF*AK1)
 0073                A(J,2)=C(J,2)*(2.-AJF*AK1)
 0074                C(J,2)=-C(J,2)*4.*AJF*AK2
              C      SLIP COEFFICIENTS NEAR THE E BOUNDARY FOR OTHER EQUATIONS
 0075         15     GO TO (16,18,19), KEX
 0076         16     CALL FRC (XD,J,INDE(J),QE)
 0077                IF (INDE(J).EQ.1) GO TO 17
 0078                AJE(J)=QE
 0079                B(J,NP2)=1.
 0080                A(J,NP2)=0.
 0081                C(J,NP2)=-8.*(1.+2.*BETA)*PREF(J)*AJE(J)/(AK*AK*BETA*(1.+BETA)*(1.
                    1+BETA)*(RHO(NP1)+3.*RHO(NP2))*U(NP1))
 0082                GO TO 20
 0083         17     F(J,NP3)=QE
 0084                B(J,NP2)=(1.+BETA-GAMA(J))/(1.+BETA+GAMA(J))
 0085                A(J,NP2)=1.-B(J,NP2)
 0086                GO TO 20
 0087         18     B(J,NP2)=(U(NP2)+U(NP1)-8.*U(NP3))/(5.*(U(NP2)+U(NP1))+8.*U(NP3))
 0088                GF=(1.-PREF(J))/(1.+PREF(J))
 0089                B(J,NP2)=(B(J,NP2)+GF)/(1.+B(J,NP2)*GF)
 0090                A(J,NP2)=1.-B(J,NP2)
 0091                GO TO 20
 0092         19     A(J,NP2)=0.
 0093                CALL SOURCE (J,NP3,CS,DS)
 0094                BK1=1./DX-DS
 0095                BK2=-BK1*F(J,NP3)-CS
 0096                BJF=BJ*PREF(J)
 0097                C(J,NP2)=1./(2.+3.*BJF*BK1)
 0098                B(J,NP2)=C(J,NP2)*(2.-BJF*BK1)
 0099                C(J,NP2)=-C(J,NP2)*4.*BJF*BK2
 0100         20     CONTINUE
 0101                RETURN
```

```
FORTRAN IV G LEVEL  20                SLIP               DATE = 72286          22/52/18

 0102            END                                                                      M 113-
```

```
FORTRAN IV G LEVEL  20                SOLVE              DATE = 72286          22/52/18

 0001            SUBROUTINE SOLVE (A,B,C,F,NP3)                                           N   1
            C    THIS SOLVES EQUATIONS OF THE FORM                                        N   2
            C    F(I) = A(I)*F(I+1) + B(I)*F(I-1) + C(I)                                  N   3
            C    FOR I=2,NP2                                                              N   4
 0002            DIMENSION A(NP3), B(NP3), C(NP3), F(NP3)                                 N   5
 0003            NP2=NP3-1                                                                N   6
 0004            B(2)=B(2)*F(1)+C(2)                                                      N   7
 0005            DO 1 I=3,NP2                                                             N   8
 0006            T=1./(1.-B(I)*A(I-1))                                                    N   9
 0007            A(I)=A(I)*T                                                              N  10
 0008       1    B(I)=(B(I)*B(I-1)+C(I))*T                                                N  11
 0009            DO 2 I=2,NP2                                                             N  12
 0010            J=NP2-I+2                                                                N  13
 0011       2    F(J)=A(J)*F(J+1)+B(J)                                                    N  14
 0012            RETURN                                                                   N  15
 0013            END                                                                      N  16-
```

```
FORTRAN IV G LEVEL  20                SOURCE             DATE = 73046          11/33/59

 0001            SUBROUTINE SOURCE (J,I,CS,DS)
 0002            COMMON /GEN/ PEI,AMI,AME,DPDX,PREF(2),PR(2),P(2),DEN,AMU,XU,XD,XP,       A   3
                1XL,DX,INTG,CSALFA,ALPHA,XR,REORS,GAM,ZETA,PPO,TWTO,YSTART,USUP,IOI       A   4
                2MEN,IHEAT,Z,TO,XSTEP/I/N,NP1,NP2,NP3,NEQ,NPH,KEX,KIN,KASE,KRAD/B/B       A   5
                3ETA,GAMA(2),TAUI,TAUE,AJI(2),AJE(2),INDI(2),INDE(2)/V/U(200),F(2,2       A   6
                4U0),R(200),RHO(200),OM(200),Y(200)/C/SC(200),AU(200),BU(200),CU(20       A   7
                50),A(2,200),B(2,200),C(2,200)/D/YR(200),UR(200),RR(200),HR(200),XM       A   8
                6(200),PITOT(200),TEMP(200)/E/DSTAR(300),XBS(300),RWRS(300),COSAL(3       A   9
                .700)                                                                     A  10
 0003            CS=SC(I)*(U(I+1)*U(I+1)-U(I)*U(I))/(OM(I+1)-OM(I))
 0004            CS=CS-SC(I-1)*(U(I)*U(I)-U(I-1)*U(I-1))/(OM(I)-OM(I-1))
 0005            CS=(1.-1./PREF(J))*CS/(OM(I+1)-OM(I-1))
 0006            DS=0.
 0007            RETURN
 0008            END
```

```
FORTRAN IV G LEVEL  20                VEFF               DATE = 72286          22/52/18

 0001            SUBROUTINE VEFF (I,IP1,EMU)                                              P   1
 0002            COMMON /GEN/ PEI,AMI,AME,OPDX,PREF(2),PR(2),P(2),DEN,AMU,XU,XD,XP,       P   2
                1XL,DX,INTG,CSALFA,ALPHA,XR,REORS,GAM,ZETA,PPO,TWTO,YSTART,USUP,IOI       P   3
                2MEN,IHEAT,Z,TO,XSTEP/V/U(200),F(2,200),R(200),RHO(200),OM(200),Y(2       P   4
                300)/I/N,NP1,NP2,NP3,NEQ,NPH,KEX,KIN,KASE,KRAD                            P   5
 0003            T=F(1,I)-U(I)**2/2.                                                      P   6
 0004            TT=F(1,IP1)-U(IP1)**2/2.                                                 P   7
 0005            T=(T+TT)/2.                                                              P   8
 0006            EMU=T**ZETA/(REORS/SQRT(2.))                                             P   9
 0007            RETURN                                                                   P  10
 0008            END                                                                      P  11-
```

```
FORTRAN IV G LEVEL  20                VISCO               DATE = 72286          22/52/18

 0001                FUNCTION VISCO (I)
 0002                COMMON /GEN/ PEI,AMI,AME,DPDX,PREF(2),PR(2),P(2),DEN,AMU,XU,XD,XP,
                    1XL,DX,INTG,CSALFA,ALPHA,XR,REORS,GAM,ZETA,PPO,TWTO,YSTART,USUP,IDI
                    2MEN,IHEAT,Z,TO,XSTEP/V/U(200),F(2,200),R(200),RHO(200),OM(200),Y(2
                    300)/I/N,NP1,NP2,NP3,NEQ,NPH,KEX,KIN,KASE,KRAD
 0003                T=F(1,I)-U(I)**2/2.
 0004                VISCO=T**ZETA/(REORS/SQRT(2.))
 0005                RETURN
 0006                END
```

```
FORTRAN IV G LEVEL  20                WALL                DATE = 72286          22/52/18

 0001                SUBROUTINE WALL
 0002                COMMON /GEN/ PEI,AMI,AME,DPDX,PREF(2),PR(2),P(2),DEN,AMU,XU,XD,XP,
                    1XL,DX,INTG,CSALFA,ALPHA,XR,REORS,GAM,ZETA,PPO,TWTO,YSTART,USUP,IDI
                    2MEN,IHEAT,Z,TO,XSTEP/V/U(200),F(2,200),R(200),RHO(200),OM(200),Y(2
                    300)/I/N,NP1,NP2,NP3,NEQ,NPH,KEX,KIN,KASE,KRAD/B/BETA,GAMA(2),TAUI,
                    4TAUE,AJI(2),AJE(2),INDI(2),INDE(2)
               C     CALCULATION OF BETA FOR THE I BOUNDARY
 0003          1     YI=.5*(Y(2)+Y(3))
 0004                UI=.5*(U(2)+U(3))
 0005                RH=.25*(3.*RHO(2)+RHO(3))
 0006                RE=RH*UI*YI/VISCO(1)
 0007                FP=DPDX*YI/(RH*UI*UI)
 0008                AM=AMI/(RH*UI)
               C     FOR LAMINAR FLOW AND AM=0 (NEED DIFFERENT EXPRESSION IF F=0)
 0009                S=1./RE-FP/2.
 0010                BETA=RE*(S+FP+AM)
 0011                TAUI=S*RH*UI*UI
 0012                IF (NEQ.EQ.1) RETURN
               C     CALCULATION OF GAMA 'S FOR THE I BOUNDARY
 0013                DO 2 J=1,NPH
               C     FOR LAMINAR FLOW AND LIMITING ZERO AM
 0014                SF=1./(PR(J)*RE)
 0015                GAMA(J)=RE*PR(J)*(SF+AM)
 0016                IF (INDI(J).EQ.1) AJI(J)=SF*RH*UI*(2.*F(J,1)-F(J,2)-F(J,3))*.5
 0017          2     CONTINUE
 0018                RETURN
 0019                END
```

APPENDIX IV
INITIAL PRESSURE DISTRIBUTION COMPUTER CODE

```
C     PROGRAM FOR INITIAL PRESSURE DISTRIBUTION
      READ (105,14) G,ALPHA,XR,XSTEP,AACT,AEFF,IDIMEN
C     G=GAMMA (RATIO OF SPECIFIC HEATS)
C     ALPHA IS DIVERGING NOZZLE WALL HALF ANGLE
C     XR IS LONGITUDINAL RADIUS OF CURVATURE OF CONVERGING SECTION
C     XSTEP IS STEP SIZE ALONG X COORDINATE (PERCENT OF LOCAL WALL RAD)
C     AACT IS THE ACTUAL NOZZLE AREA RATIO
C     AEFF IS THE EFFECTIVE NOZZLE AREA RATIO
C     IDIMEN=0 FOR TWO-DIMENSIONAL NOZZLE AND 1 FOR AXISYMMETRIC NOZZLE
C     XWIG, ZWIG, AND RWIG ARE THE COORDINATES OF THE POINT WHERE THE
C     NOZZLE WALL SLOPES ARE MATCHED JUST DOWNSTREAM OF THE THROAT
      ALPHA=ALPHA*3.14159/180.
      NUM=0
      PI2=3.14159/2.
      COSALF=COSF(ALPHA)
      SINALF=SINF(ALPHA)
      ZWIG=XR*(1.+SINALF)
      XWIG=XR*(PI2+ALPHA)
      RWIG=1.+XR*(1.-COSALF)
      XTHOAT=XR*PI2
      REND=SQRTF(AACT)
      IF (IDIMEN.EQ.0) REND=AACT
      XEND=XWIG+(REND-RWIG)/SINALF
      CONST=(SQRTF(AACT)-SQRTF(AEFF))/(COSALF*(XEND-XWIG)**1.5)
      IF (IDIMEN.EQ.0) CONST=(AACT-AEFF)/(COSALF*(XEND-XTHOAT))
      ALPHA=ALPHA*180./3.14159
      IF (IDIMEN.EQ.0) WRITE(108,18)
      IF (IDIMEN.EQ.1) WRITE(108,19)
      WRITE (108,15) G,ALPHA,XR,XEND,XSTEP,AACT,AEFF
      C1=(G+1.)/2.
      C2=(G-1.)/2.
      C3=C1/(G-1.)
      C4=C1**C3
      C5=C4*C2*C3*2.
      FM=0.5
      X=0.0
      R=0.0
      DS=0.0
    1 CONTINUE
      XU=X
      X=X+XSTEP*R
      IF (X-XWIG) 2,2,4
    2 CONTINUE
      IF (.NOT.(XU.LT.XTHOAT.AND.X.GT.XTHOAT)) GO TO 3
      X=XTHOAT
    3 CONTINUE
      Z=XR*(1.0-COSF(X/XR))
      R=1.+XR*(1.-SINF(X/XR))
      RINV=R
      COSA=SINF(X/XR)
      GO TO 5
    4 Z=(X-XWIG)*COSALF+ZWIG
      R=(X-XWIG)*SINALF+RWIG
      COSA=COSALF
```

```
      DS=CONST*(X-XWIG)**1.5
      IF (IDIMEN.EQ.0) DS=CONST*(X-XWIG)
      RINV=R-DS*COSALF
 5    A=(1./RINV)**(1+IDIMEN)
      IF (A-1.0) 7,6,6
 6    A=1.0
      FM1=1.0
      FM=1.0
      B=1.0+C2
      GO TO 12
 7    IF (X-PI2*XR) 11,11,9
 8    B=(1.+C2*FM1**2)
      FM=FM1-(A*B**(C3+1.)-C4*FM1)/(C5*FM1**2-C4)
      IF (ABS(FM-FM1)-0.00001) 12,11,11
 9    CONTINUE
      IF (FM-1.20) 10,11,11
 10   FM=1.20
 11   FM1=FM
      GO TO 8
 12   CONTINUE
      POP=B**(G/(1.-G))
      NUM=NUM+1
      Z=Z-XR
      WRITE (108,16) FM,POP,Z,X,DS,R,RINV,NUM
      WRITE (106,17) X,POP,NUM
      IF (X-XEND) 1,1,13
 13   CONTINUE
      STOP
C
 14   FORMAT(6E10.0,I1)
 15   FORMAT(10X,'GAMMA =',F7.3/,10X,
     2'ALPHA =',F7.3/,10X,'XR      =',F7.3/,10X,'XEND   =',F7.3/,10X,'XSTEP
     3 =',F7.3/,10X,'AACT   =',F7.3/,10X,'AEFF   =',F7.3///,8X,'M',11X,
     4'P/PO',12X,'Z',13X,'X',12X,'DS',12X,'RW',11X,'RINV',7X,'NUM'/)
 16   FORMAT(1P7E14.5,I6)
 17   FORMAT(2E12.6, 53X, I3)
 18   FORMAT(1H1,9X,   'ONE-DIMENSIONAL PERFECT GAS EXPANSION FOR A TWO-
     1DIMENSIONAL NOZZLE GEOMETRY WITH'/,10X,'THE ASSUMPTION THAT THE BO
     2UNDARY-LAYER DISPLACEMENT THICKNESS VARIES AS (X-XWIG)'//)
 19   FORMAT(1H1,9X,'ONE-DIMENSIONAL PERFECT GAS EXPANSION FOR AN AXISYM
     1METRIC NOZZLE GEOMETRY WITH THE'/,     10X,'ASSUMPTION THAT THE BO
     2UNDARY-LAYER DISPLACEMENT THICKNESS VARIES AS (X-XWIG)**3/2'//)
      END
```

UNCLASSIFIED

Security Classification

DOCUMENT CONTROL DATA - R & D

(Security classification of title, body of abstract and indexing annotation must be entered when the overall report is classified)

1 ORIGINATING ACTIVITY (Corporate author) Arnold Engineering Development Center Arnold Air Force Station, Tennessee 37389	2a. REPORT SECURITY CLASSIFICATION UNCLASSIFIED 2b GROUP N/A

3 REPORT TITLE

VISCOUS EFFECTS IN LOW-DENSITY NOZZLE FLOWS

4 DESCRIPTIVE NOTES (Type of report and inclusive dates)

March 9 to November 30, 1972--Final Report

5 AUTHOR(S) (First name, middle initial, last name)

David L. Whitfield, ARO, Inc.

6 REPORT DATE	7a. TOTAL NO OF PAGES	7b. NO OF REFS
June 1973	77	18

8a. CONTRACT OR GRANT NO. b. PROJECT NO. c. Program Element 62302F d.	9a. ORIGINATOR'S REPORT NUMBER(S) AEDC-TR-73-52 9b. OTHER REPORT NO(S) (Any other numbers that may be assigned this report) ARO-VKF-TR-73-8

10 DISTRIBUTION STATEMENT

Approved for public release; distribution unlimited.

11 SUPPLEMENTARY NOTES	12. SPONSORING MILITARY ACTIVITY
Available in DDC	AFRPL/DYSP Edwards Air Force Base California 93523

13 ABSTRACT

Viscous effects in low-density nozzle flows were investigated numerically, and comparisons were made with experimental data. The numerical method of Patankar and Spalding was modified to solve the internal laminar boundary-layer equations for two-dimensional flow or axisymmetric flow with or without transverse curvature. A listing is given of the computer code. Boundary-layer displacement thicknesses for typical nozzle geometries and flow conditions are presented. Solutions were obtained for specific conditions corresponsing to experimental data. The result is a relatively fast, simple to use numerical procedure, which is shown to give results in good agreement with experimental data.

DD FORM 1 NOV 65 1473

UNCLASSIFIED

Security Classification

14. KEY WORDS	LINK A		LINK B		LINK C	
	ROLE	WT	ROLE	WT	ROLE	WT
test facilities						
convergent divergent nozzles						
rocket nozzle						
scaling						
low density						
wind tunnels						
numerical analysis						

AFSC
Arnold AFB Tenn